Mass Spectrometric Studies of the Mechanisms of Two Halo Acid Dehalogenases(Dissertation_全文)

AUTHOR(S):

Ichiyama, Susumu

Mass Spectrometric Studies of the Mechanisms of Two Halo Acid Dehalogenases

Susumu Ichiyama

2000

Mass Spectrometric Studies of the Mechanisms of Two Halo Acid Dehalogenases

Susumu Ichiyama

2000

CONTENTS

LIST OF FIGURES, SCHEMES, AND A TABLE

ABBREVIATIONS

amu	atomic mass unit(s)
β-CNAla	β-cyano-L-alanine
BpoA2	bromoperoxidase A2 from *Streptomyces aureofaciens*
4-CBA-CoA	4-chlorobenzoyl-coenzyme A
DhlA	haloalkane dehalogenase from *Xanthobacter autotrophicus* GJ10
DL-DEX	DL-2-Halo acid dehalogenase
DL-DEX 113	DL-2-Halo acid dehalogenase from *Pseudomonas* sp. 113
FAc-DEX	fluoroacetate dehalogenase from *Moraxella* sp. B
HPLC	high performance liquid chromatography
LB	Luria Bertani
L-CPA	L-2-chloropropionic acid or L-2-chloropropionate
L-DEX YL	L-2-halo acid dehalogenase from *Pseudomonas* sp. YL
MEH	rat liver microsomal epoxide hydrolase
MS	mass spectrometry
PAGE	polyacrylamide gel electrophoresis
PCR	polymerase chain reaction
PTH	phenylthiohydantoin
SDS	sodium dodecyl sulfate
TPCK	*N*-tosyl-L-phenylalanyl chloromethyl ketone

GENERAL INTRODUCTION

Halogenated organic compounds containing fluorine, chlorine, bromine, and iodine are synthesized by various organisms such as marine and terrestrial plants, fungi, and bacteria (1–5). Many of these compounds have antibacterial, antifungal, or herbicidal activity.

Halogenated compounds have been produced also by man and widely used for many purposes as paint removers, refrigerants, cleaning solvents, herbicides, etc. Dichlorodiphenyltrichloroethane (DDT) was the first widely-used chlorinated organic compound. It was used extensively throughout the world as a very effective insecticide. However, it was condemned later because it accumulates and persists in the fatty tissue of animals due to its insolubility in water and solubility in nonpolar hydrocarbons. Like DDT, many of the halogenated compounds accumulate in the biosphere due to their persistence, and cause problems because of their toxicity, teratogenicity, and carcinogenicity (6, 7). Many kinds of halogenated compounds are now detected almost anywhere such as in surface and ground water, food, and the atmosphere (8).

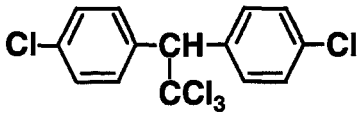

DDT

A group of halogenated organic compounds of particular concern are the chlorofluoromethanes and -ethanes, which are generally called flons. These compounds were developed as refrigerant gases. Freon 11 and 12 have been used as the propellant for the production of aerosol spray cans. When these fluorinated compounds are released into the atmosphere, they accumulate in the stratosphere and are decomposed photochemically by sunlight to generate free chlorine radicals, which are believed to catalyze the decomposition of ozone (9). Since ozone cuts out the ultraviolet rays from sunlight, decrease in the ozone concentration increases the radiation of harmful short-wavelength rays to the surface of the earth (10, 11).

Cl_3CF	Cl_2CF_2
Fluorotrichloromethane	**Dichlorodifluoromethane**
(Freon 11)	**(Freon 12)**

Concerns about the influence of halogenated organic compounds have increased the interest in the development of remediation technologies. Microorganisms that can degrade halogenated organic compounds as a growth substrate have been isolated from various sources such as activated sludge and soil. These microorganisms generally produce dehalogenases, which catalyze the carbon–halogen bond cleavage. With the aim of obtaining enzymes with improved catalytic activity for detoxification of organohalogen compounds, intensive studies including kinetic studies, site-directed

mutagenesis, mass spectrometry (MS), and X-ray crystallography have been carried out to clarify the detailed mechanisms and the structures of dehalogenases.

L-2-Halo acid dehalogenase (L-DEX; EC 3.8.1.2) catalyzes the hydrolytic dehalogenation of L-2-haloalkanoates to produce the corresponding D-2-hydroxyalkanoates, with inversion of the configuration at the C2 atom (12). L-DEXs are utilized as industrial biocatalysts in the synthesis of chiral compounds based on their stereospecificity (13). L-DEX YL, isolated from a 2-chloroacrylate-utilizable bacterium, *Pseudomonas* sp. YL, is a unique L-DEX in that it is quite thermostable even though it is derived from a mesophilic bacterium (14). It is a dimeric enzyme composed of two identical subunits. Kurihara et al. mutated all polar and charged amino acid residues of L-DEX YL which are conserved among L-DEXs, and identified Asp-10, Thr-14, Arg-41, Ser-118, Lys-151, Tyr-157, Ser-175, Asn-177, and Asp-180 as catalytically important residues (15). Ion-spray mass spectrometric studies showed that the dehalogenation catalyzed by L-DEX YL proceeds through a two-step mechanism: a nucleophile Asp-10 attacks the C2 atom of the substrate causing the release of a halide ion and formation of an ester intermediate, which is subsequently hydrolyzed to produce a D-2-hydroxyalkanoate as shown in Scheme 1A, in which X represents a halogen atom other than fluorine (16). The first step has been further investigated by mass spectrometric analyses of the enzyme paracatalytically modified by hydroxylamine: the enzyme forms an adduct of the dehalogenated substrate moiety and hydroxylamine specifically at the Asp-10 position, supporting the formation of the ester intermediate between Asp-10 and the substrate (17). The enzyme has also been studied by X-ray crystallography (18). The enzyme has an α/β-structure as a core do-

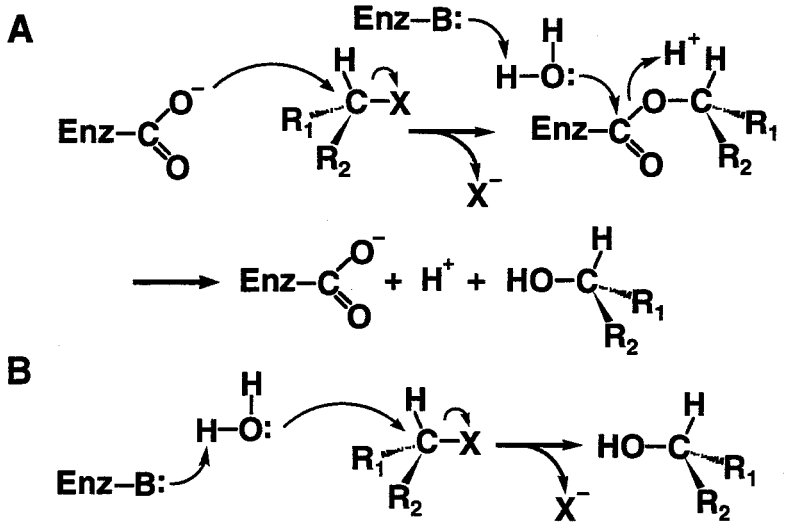

Scheme 1. **Two possible mechanisms for hydrolytic dehalogenation.** *A*, a two-step mechanism through an ester intermediate formed from an acidic amino acid residue serving as a nucleophile and a substrate. The ester is then hydrolyzed by a water molecule. *B*, a one-step mechanism for a concerted nucleophilic substitution caused by a water molecule which is activated by a base of the enzyme.

main which topologically differs from the structure of α/β hydrolase fold family proteins (19), along with a subdomain having a four-helix-bundle structure. The X-ray structure of L-DEX YL S175A complexed with various L-2-chloroalkanoates has provided us with insights in the steps of the catalytic process (20). The carboxyl oxygens of the substrate are hydrogen-bonded with the Ser-118 hydroxyl group and the main-chain amido-nitrogens of Leu-11, Tyr-12, and Asn-119. The hydrophobic pocket, which is mainly composed of side chains of Tyr-12, Gln-42, Leu-45, Phe-60, Lys-151, Asn-177, and Trp-179, exists around the alkyl group of the substrate. This pocket probably plays an important role in stabilizing the alkyl group of the substrate through hydrophobic interactions, and, along with Ser-118 fixing the carboxyl group of the substrate, also plays a role in determining the stereospecificity of the enzyme. In the second step of the reaction, the ester bond is hydrolyzed by a nucleophilic attack of a water molecule probably activated by Ser-175, Asn-177, and Asp-180 (21). The guanidino group of Arg-41 most likely serves as the halogen abstraction site.

The reactions catalyzed by haloalkane dehalogenase (EC 3.8.1.5) from *Xanthobacter autotrophicus* GJ10 (DhlA) (22), and 4-chlorobenzoyl-coenzyme A (4-CBA-CoA) dehalogenases (EC 3.8.1.7) from *Pseudomonas* sp. CBS3 (23) and *Arthrobacter* sp. 4-CB1 (24) also proceed through mechanisms similar to that of L-DEX YL involving the formation of an enzyme–substrate ester intermediate. DhlA and 4-CBA-CoA dehalogenase belong to different families of proteins from each other and also from L-DEX (25). In the study of the DhlA reaction mechanism, a series of soaking experiments of crystals provided evidence for formation of an ester intermediate formed between a nucleophile Asp-124 and the C1 atom of the substrate (26). Different stages such as acceptance of a halide ion by Trp-125 and Trp-175, and hydrolysis of the ester intermediate in the reaction pathway could also be trapped by changing the pH and temperature of the solution. Site-directed mutagenesis and ^{18}O-incorporation experiment confirmed that Asp-124 functions as the nucleophile to attack the substrate (22). Site-directed mutagenesis of the prospective base His-289 and the two halide-accepting residues Trp-125 and Trp-175 showed the essential role of these amino acid residues in activating the water molecule and binding of a halide ion, respectively (27, 28). From stopped-flow fluorescence analyses of DhlA, Schanstra et al. proposed that a conformational change in the cap domain occurred to allow water to enter the active site and solvate the halide ion, and concluded that the halide release is the rate-limiting step of the reaction (29).

DL-2-Halo acid dehalogenase (DL-DEX; EC 3.8.1.2) catalyzes dehalogenation of both D- and L-2-haloalkanoates to produce the corresponding L- and D-2-hydroxyalkanoates, respectively. DL-DEX acts indiscriminately on the chiral center of both D- and L-enantiomers, and catalyzes a chemical conversion on the chiral centers of both enantiomers. Nardi-Dei et al. showed by site-directed mutagenesis and ^{18}O-

incorporation experiments that the reaction catalyzed by DL-DEX from *Pseudomonas* sp. 113 (DL-DEX 113) proceeds as shown in Scheme 1B: a water molecule is probably activated by a single catalytic base of the enzyme and directly attacks the α-carbon of D- and L-2-haloalkanoates to displace a halogen atom (30, 31).

None of the enzymes described above catalyzes the hydrolytic cleavage of a C–F bond, because the dissociation energy of the C–F bond of aliphatic fluorocompounds is among the highest found in natural products (32). Exceptionally, fluoroacetate dehalogenases (EC 3.8.1.3) from a few *Pseudomonas* strains and a *Moraxella* strain catalyze the hydrolytic cleavage of a C–F bond of fluoroacetate (33–36). Fluoroacetate dehalogenase from *Moraxella* sp. B (FAc-DEX) most preferentially catalyzes defluorination of fluoroacetate, along with dehalogenation of other haloacetates.

In order to clarify the catalytic mechanism of FAc-DEX and to compare the mechanism with that of L-DEX YL, which shows no defluorination activity, the author has carried out mass spectrometric studies of FAc-DEX and L-DEX YL. In Chapter I, the author identified amino acid residues participating in the reaction and determined the catalytic mechanism that involves an ester intermediate by site-directed mutagenesis and ion-spray mass spectrometry. Chapter II deals with paracatalytic inactivation of FAc-DEX by hydroxylamine and ammonia. It is a distinctive feature that ammonia, which is a weak nucleophilic reagent compared with hydroxylamine and does not inactivate L-DEX YL, acts as a paracatalytic inhibitor by attacking on the ester intermediate of FAc-DEX reaction. Chapter III describes spontaneous hydrolytic deamidation of Asn-105 of FAc-DEX D105N mutant enzyme. Chapter IV presents a novel property of Asn residue revealed by analyzing the reaction mechanism of L-DEX YL D10N mutant enzyme. Asn-10 of L-DEX YL D10N nucleophilically attacks α-carbon of the substrate to cleave the carbon–halogen bond.

By means of site-directed mutagenesis and mass spectrometric analyses, the author clarified the catalytic mechanisms of the two dehalogenases, FAc-DEX and L-DEX YL, which have little sequence similarity with each other. The investigation presented in this thesis should provide insights into general understanding of the mechanism of hydrolases.

CHAPTER I

Reaction Mechanism of Fluoroacetate Dehalogenase from *Moraxella* sp. B

INTRODUCTION

Fluoroacetate is one of the most toxic compounds for mammals (37). Its toxicity is due at least partly to its conversion to (2*R*,3*R*)-*erythro*-2-fluorocitrate by citrate synthase (EC 4.1.3.7); the latter compound is a strong inhibitor of aconitase (EC 4.2.1.3). An X-ray crystallographic analysis of the enzyme–inhibitor complex has revealed that 4-hydroxy-*trans*-aconitate formed from (2*R*,3*R*)-*erythro*-2-fluorocitrate is tightly bound to the enzyme (38). Some plants found in Australia, Africa, and Central America synthesize high concentrations of fluoroacetate from fluoride (4). Tamura et al. (5) have shown that fluoroacetate is synthesized in *Streptomyces cattleya* from fluoride and β-hydroxypyruvate.

The dissociation energy of a C–F bond of aliphatic fluorocompounds is among the highest found in natural products (32). Various dehalogenases, *e.g.* L-DEX YL (16), DhlA (22), and 4-CBA-CoA dehalogenases (23, 24) have been characterized. However, none of them catalyze the hydrolytic cleavage of the C–F bond.

Fluoroacetate dehalogenases, which catalyze hydrolytic defluorination of fluoroacetate, have been demonstrated in a few *Pseudomonas* strains and characterized (33–35). Kawasaki et al. have isolated a *Moraxella* strain producing FAc-DEX (36) and have cloned its gene in *Escherichia coli* (39). Two probable mechanisms can be delineated for the enzyme reaction (40). One of them (Scheme 2A) is similar to that of DhlA as shown by X-ray crystallography: an aspartate residue at the active site acts as a nucleophile causing the release of a halide ion and the for-

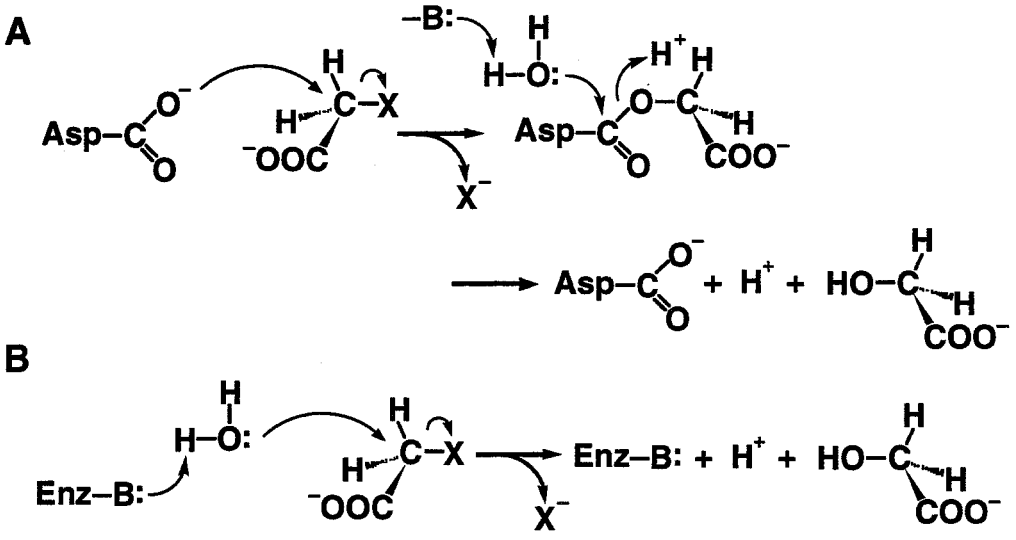

Scheme 2. **Possible mechanisms for the FAc-DEX reaction.**

mation of an ester intermediate, which is subsequently hydrolyzed by a water molecule activated by a histidine residue (26). Recently the reaction catalyzed by rat liver microsomal epoxide hydrolase (MEH) (EC 3.3.2.3) has also been shown to proceed via an ester intermediate: Asp-226 and His-431 act as a nucleophile and a base, respectively (41, 42). The amino acid sequence of FAc-DEX is similar to that of DhlA (identity 18%) and MEH (identity 14%). Moreover, Asp-124 and His-289 of DhlA and Asp-226 and His-431 of MEH serving as the nucleophile and the base are conserved as Asp-105 and His-272, respectively, in FAc-DEX. Therefore, one can speculate that the mechanism of FAc-DEX is similar to that of DhlA and MEH. However, in another probable mechanism shown in Scheme 2B, a water molecule is activated by a catalytic base of the enzyme and directly attacks the α-carbon of a haloacetate to displace the halogen atom. The reaction catalyzed by DL-DEX 113 has been shown to proceed through this mechanism (31, 43). Although little sequence similarity is found between FAc-DEX and DL-DEXs, the FAc-DEX reaction could possibly follow the same mechanism as DL-DEX.

I have purified and characterized FAc-DEX to clarify its catalytic mechanism by site-directed mutagenesis and ion-spray mass spectrometry. I show here that the reaction proceeds through the mechanism shown in Scheme 2A, and that Asp-105 and His-272 act as the nucleophile and the base, respectively.

EXPERIMENTAL PROCEDURES

Materials—Sodium fluoroacetate was purchased from Wako Pure Chemical Industries (Osaka, Japan), trypsin and chloroacetic acid from Nacalai Tesque (Kyoto, Japan), DEAE-Toyopearl from Tosoh (Tokyo), Gigapite from Toagosei Chemical Industry (Tokyo), Superose 12HR from Amersham Pharmacia Biotech (Uppsala, Sweden), $H_2{}^{18}O$ (95–98%) from Cambridge Isotope Laboratories (Andover, MA) or Nippon Sanso (Tokyo), deuterium oxide (D_2O) from Euriso-top (Gif sur Yvette, France), and [1-^{14}C]chloroacetic acid (4.4×10^8 Bq/mmol, 3.3×10^7 Bq/ml in toluene) from Sigma (St. Louis, MO). Other chemicals were of analytical grade.

DNA Techniques—General procedures for DNA manipulations were carried out as described previously (44). The 1.5-kb *Sal*I–*Kpn*I fragment including the FAc-DEX gene was isolated from the recombinant plasmid pBREF1 (45) and then amplified by polymerase chain reaction (PCR), with *Hin*dIII sites being introduced to both ends of the PCR-amplified structural gene: the restriction sequences for *Hin*dIII (AAGCTT) were introduced in the region from 59 to 64 nucleotides upstream of the initiation codon ATG, and in the region from 58 to 63 nucleotides downstream of the termination codon TGA (at position 943 to 948 from the initiation codon). The synthetic mutagenic primers used were as follows (underlines indicate the mutagenized nucleotides):

forward primer, 5'-CTCA-AGCTTAAGGGTGAACGTGGCTG;
reverse primer, 5'-CTCAAGCTTGCCCTCTCTCTAGCGTT.
The resultant DNA was ligated to the *Hin*dIII-digested pUC119 to yield pUCH-1. The plasmid pUCH-1 contained an insert of about 1 kbp. The nucleotide sequence of the FAc-DEX gene in pUCH-1 was identical to that of the original one in pBREF1 except for two bases: G substituted for A at position 244, which led to an alteration from Thr to Ala, and T substituted for C at position 390, which gave a different codon for the same amino acid, Ile. The recombinant plasmid pUCH-1 encoding FAc-DEX was mutagenized by the method of Kunkel (46). The synthetic mutagenic primers used were as follows (underlines indicate the mutagenized nucleotides):
D105A, 5'-GCGAGCATGTCC;
D105G, 5'-GCGACCATGTCC;
D105V, 5'-GCGAACATGTCC;
R106G, 5'-GCCGCCATCATGTCC;
R106K, 5'-GGTACGCCCGCCTTTATCATGTCCGACGAG;
R106S, 5'-GCCGCTATCATGTCC;
R106W, 5'-CCCGCCCCAATCATGTCCGACG;
H272N, 5'-GAAGAAATTGCCTCCTG;
H272D, 5'-GAAGAAATCGCCTCCTG;
H272Y, 5'-GAAGAAATAGCCTCCTG.
The substitutions were confirmed by DNA sequencing with a Dye Terminator sequencing kit and an Applied Biosystem 370A DNA sequencer. Mutant enzymes were produced in *E. coli* JM109.

Enzyme Purification—All operations were performed at 4°C, and 50 mM potassium phosphate (pH 7.5) was used as the standard buffer unless otherwise stated. *E. coli* JM109 cells were grown aerobically at 37°C for 14 h in 1 liter of Luria Bertani (LB) medium containing 200 μg/ml ampicillin, 0.2 mM isopropyl-1-thio-β-D-galactoside, and 0.1 mg/ml bromoacetate. The cells were harvested, rinsed with the standard buffer, and suspended in 20 ml of the same buffer. The cell suspension was subjected to ultrasonic oscillation at 4°C for 25 min with a Seiko Instruments model 7500 ultrasonic disintegrator, followed by centrifugation at 12,000 rpm for 15 min. The supernatant was fractionated with ammonium sulfate, and the precipitate formed between 40–70% saturation of the salt was dissolved in the standard buffer, dialyzed against the same buffer, and subsequently applied to a DEAE-Toyopearl 650M column (3 × 27 cm). The elution was carried out with a linear gradient of 50–300 mM potassium phosphate (pH 7.5). The active fractions were pooled, dialyzed against 10 mM potassium phosphate (pH 7.5), and applied to a Gigapite column (1 × 13 cm). The elution was carried out with a linear gradient of 10–300 mM potassium phosphate (pH 7.5). The active fractions were pooled and used as the purified enzyme.

Determination of Enzyme Activity and Protein—FAc-DEX was routinely assay-

ed by determination of chloride ions produced from chloroacetate by the method of Iwasaki et al. (47). Glycolate produced from fluoroacetate and other haloacetates was determined by high performance liquid chromatography (HPLC): column, Millipore Puresil 5 μ C_{18} 120 Å, 4.6 × 150 mm; elution, 0.05% trifluoroacetic acid; detection, absorption at 215 nm. The standard assay mixture (100 μl) contained 2.5 μmol of sodium chloroacetate (or other haloacetate), 10 μmol of Tris-sulfate buffer (pH 9.5), and the enzyme. The reaction was terminated by addition of 10 μl of 1.5 M sulfuric acid after incubation at 30°C for 10 min. One unit of the enzyme was defined as the amount of the enzyme that catalyzes dehalogenation of 1 μmol of chloroacetate per min. Protein concentration was determined with a Bio-Rad protein assay kit.

Determination of Molecular Masses of FAc-DEX—FAc-DEX (10 nmol) dissolved in the 5.3 μl of the standard buffer was mixed with 84.7 μl of H_2O or D_2O containing 10 μmol of Tris-sulfate (pH 9.5) and 2.5 μmol of fluoroacetate, and incubated at 30°C for indicated times shown in Fig. 5 (p.15). The reaction was terminated with 10 μl of 20% (v/v) formic acid, followed by centrifugation at 8200 *g* for 1 min. The enzyme was deionized with Jasco HPLC system (Tokyo) with a C_{18} reverse phase column (Shiseido Capcell Pak, SG 300 Å 5 μm, 4.6 × 250 mm) at room temperature, employing linear gradients of solvent A (0.1% formic acid) and solvent B (acetonitrile containing 0.1% formic acid): sample injection; 3 min, 20% B; 12 min, 20–100% B; 3 min, 100% B; 2 min, 100–20% B (flow rate: 1 ml/min). The deionized enzyme was lyophilized, dissolved in 50% acetonitrile containing 0.05% formic acid, and introduced into a mass spectrometer, PE-Sciex API 3000 (Sciex, Thornhill, Ontario, Canada) at a flow rate of 2.5–5 μl/min. The quadrupole was scanned from 800 to 2,000 atomic mass units (amu) with a step size of 0.2 amu and with a dwell time of 1 ms/step. The ion-spray voltage was set at 5 kV, and the orifice potential was set at 60 V.

Reaction of FAc-DEX in $H_2{}^{18}O$, Digestion of ^{18}O-Labeled Enzyme with Trypsin, and LC/MS Analysis of the Resultant Peptides—FAc-DEX (10 nmol) was lyophilized. The dried enzyme was dissolved in 50 μl of $H_2{}^{18}O$ containing 1 μmol of sodium fluoroacetate and 20 μmol of Tris-sulfate (pH 9.5), and the mixture was incubated at 30°C for 12 h. Fluoroacetate was omitted in a control experiment. The reaction was stopped by the addition of 100 μl of 5 M urea solution in $H_2{}^{18}O$ and was followed by incubation at 37°C for 1 h. The enzyme was then digested with 5 μg of trypsin at 37°C for 12 h. The proteolysate was loaded onto a packed capillary perfusion column (Poros II R/H, 320 μm × 10 cm, LC Packings, San Francisco, CA) connected to a mass spectrometer, PE-Sciex API *III*, equipped with an ion-spray ion source, and elution was then carried out with a linear gradient of 0–80% acetonitrile in 0.05% trifluoroacetic acid over 40 min at a flow rate of 10 μl/min. The total ion current chromatogram was recorded in the single-quadrupole mode with the mass spectrometer. The quadrupole was scanned from 300 to 2,000 amu with a step size of

0.25 amu and with a dwell time of 0.5 msec/step. The orifice potential was 80 V. The molecular mass of each peptide was calculated with MacSpec software supplied by PE-Sciex. The HPLC fractions were collected, concentrated, and injected into the mass spectrometer for tandem MS/MS analysis described below.

Tandem MS/MS Analysis of the Peptides Containing Asp-105—The MS/MS daughter ion spectra were obtained in the triple-quadrupole daughter ion scan mode by selectively introducing the peptides containing Asp-105 (*m/z* 984.8 or 980.8) from Q1 into a collision cell (Q2) and observing the daughter ions in Q3. Q1 was locked on *m/z* 984.8 or 980.8. Q3 was scanned from 50 amu to just above the molecular weight of the peptides with a step size of 0.1 amu and with a dwell time of 1 msec/step. The orifice potential was 100 V. The collision energy was 30 eV.

Labeling of H272N with [^{14}C]Chloroacetate—Commercially available [1-^{14}C]chloroacetic acid is dissolved in toluene. It has been confirmed that the FAc-DEX activity is not affected by toluene when suspended in a reaction mixture at a ratio of 10% (v/v). The reaction mixture containing 10 μmol of Tris-sulfate (pH 9.5), 0.75 μmol of sodium hydroxide, the wild-type enzyme or H272N (1 mg each), and 10 μl of toluene solution containing [1-^{14}C]chloroacetic acid in a final volume of 100 μl was incubated at 30°C for 2 h. The reaction mixture was dialyzed against the standard buffer for 14 h and then applied to the C_{18} reverse phase HPLC column. The elution was carried out with 0.05% trifluoroacetic acid for 5 min, followed by a linear gradient of 0–80% acetonitrile in 0.05% trifluoroacetic acid as described above. The radioactivity of the eluate was determined with a Packard Tri-Carb scintillation spectrometer with Clear-sol I (Nacalai Tesque, Kyoto, Japan) as a scintillator.

MS Analysis of H272N and Its Proteolytic Peptides—H272N (400 μg) previously lyophilized was dissolved in a mixture (40 μl) containing 0.5 M Tris-sulfate (pH 9.5) and 125 mM sodium fluoroacetate, and the solution was incubated at 30°C for 2 h. Fluoroacetate was omitted in a control experiment. A solution of 5 M urea (100 μl) was added to the mixture, and the solution was further incubated at 37°C for 1 h. The enzyme was then digested with 5 μg of trypsin at 37°C for 12 h. The resultant peptide fragments were applied to the capillary column connected to the ion-spray mass spectrometer as described above.

RESULTS

Purification of FAc-DEX from Recombinant E. coli Cells—FAc-DEX was purified to homogeneity (Table I). The purity of the final preparation was judged by sodium dodecyl sulfate polyacrylamide gel electrophoresis (SDS-PAGE) (data not shown). The molecular weight of the enzyme was determined to be about 67,000 by Superose 12HR gel filtration chromatography in a native state, whereas it was about 33,000 by SDS-PAGE. Therefore, the enzyme appears to be composed of two identical subunits. The enzyme had a maximum activity at pH 9.5 and was stable in

TABLE I
Purification of FAc-DEX

Step	Total protein (mg)	Total activity (units)	Specific activity (units/mg)	Purification (-fold)	Yield (%)
Crude Extract	330	726	2.2	1	100
Ammonium Sulfate Precipitation	125	710	5.7	2.6	98
DEAE-Toyopearl	32.5	426	13	5.9	59
Gigapite	14.5	260	18	8.2	36

The enzyme was purified as described in "Experimental Procedures." The dehalogenase activities of pooled fractions were determined by measuring the chloride ions released from 25 mM chloroacetate.

the pH range from 6.0 to 10.0. The highest enzyme activity in terms of initial velocities was observed at 50°C, but 70% of the initial activity was lost upon incubation of the enzyme at this temperature for 30 min. The relative activities for several haloacetates were as follows: fluoroacetate, 480; chloroacetate, 100; bromoacetate, 60; iodoacetate, 2.6; dichloroacetate, 1.0. The following halogen compounds were inert: trichloroacetate, 2-chloropropionate, chloroethane, 2-chloroacetamide, and chloromethane. Glycolate was produced from monohaloacetates by dehalogenation, and it inhibited the enzyme at concentrations higher than 10 mM. These properties are similar to those reported for the *Pseudomonas* enzymes (33, 35).

Site-Directed Mutagenesis of Asp-105, Arg-106, and His-272 of FAc-DEX—The sequence analysis of DhlA (48) showed that it has around 18% similarity with FAc-DEX, suggesting structural and mechanistic similarities (Fig. 1). In particular, the regions around the nucleophilic aspartate residue and the base histidine residue of DhlA are conserved as Asp-105 and His-272, respectively, in FAc-DEX (Fig. 1). Arg-106 of FAc-DEX corresponds to one of the halogen binding residues of DhlA, Trp-125 (Fig. 1). Asp-105 was replaced by Ala, Gly, and Val; Arg-106 by Gly, Lys, Ser, and Trp; and His-272 by Asn, Asp, and Tyr by site-directed mutagenesis. All mutant enzymes were highly expressed in *E. coli* (about 5–10% of the total amount of soluble cellular proteins). However none of them showed dehalogenation activity, indicating that Asp-105, Arg-106, and His-272 of FAc-DEX play essential roles in catalysis.

^{18}O-Labeling of the Enzyme and Isolation of the Labeled Peptide—If Asp-105 of FAc-DEX acts as a nucleophile as shown in Scheme 2A (p.5), the carboxyl group of the residue is expected to be labeled with ^{18}O when the enzymatic defluorination of fluoroacetate is carried out in $H_2{}^{18}O$. Therefore, the reaction in $H_2{}^{18}O$ was performed as described in "Experimental Procedures." The enzyme was then digested with trypsin, and the resultant peptide fragments were separated and analyzed by ion-spray mass spectrometry. When the spectrometer was in the single-quadrupole mode, the

total ion current chromatogram displayed several peaks: one could clearly be assigned to be an octapeptide Phe-99–Arg-106 containing Asp-105 (data not shown). This peptide was isolated by reverse phase HPLC and sequenced with a Shimadzu protein sequencer PPSQ-10 (Kyoto, Japan), giving the following sequence: Phe–His–Leu–Val–Gly–His–Asp–Arg, which is identical to that predicted from the nucleotide sequence. Ion-spray mass spectrometry of the octapeptide derived from the native

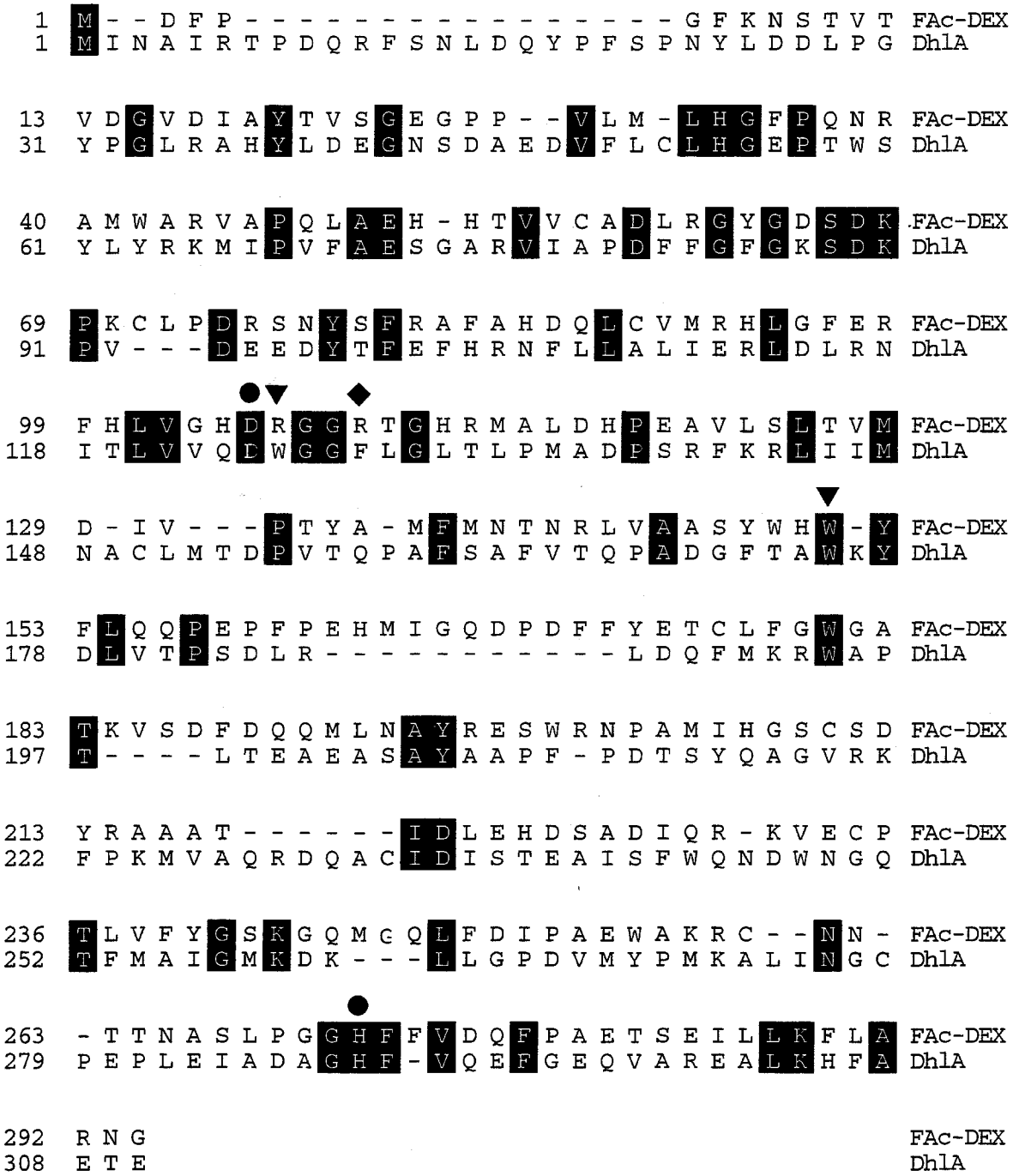

FIG. 1. **Amino acid sequence alignment of FAc-DEX and DhlA (48).** The sequence similarity was examined with the program MegAlign (DNASTAR Inc., Madison, WI). The conserved residues are shaded. Numbers on the left indicate the residue numbers in each amino acid sequence. Symbols are as follows: (●), the conserved aspartate and histidine residues; (▼), Cl-1 atom binding residues of DhlA; (◆) Cl-2 atom binding residue of DhlA.

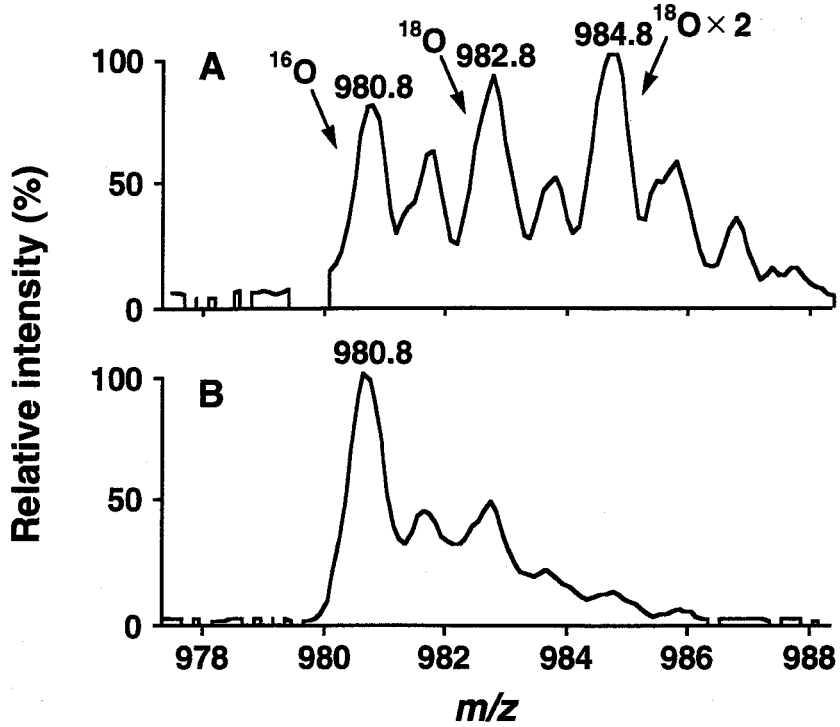

FIG. 2. **Ion-spray mass spectra of the peptides containing Asp-105.** Mass spectrum of the octapeptide Phe-99–Arg-106 derived from the enzyme incubated in $H_2{}^{18}O$ with (A) or without (B) fluoroacetate are shown.

enzyme showed a peak at *m/z* 980.8, which was assigned as the $[M + H]^+$ ion based on the calculated mass (979.5) of the octapeptide (data not shown). The octapeptide isolated from the enzyme incubated with fluoroacetate in $H_2{}^{18}O$ showed two new $[M + H]^+$ peaks at *m/z* 982.8 and 984.8 (Fig. 2A). However, when fluoroacetate was omitted from the reaction mixture in $H_2{}^{18}O$, only the peak at *m/z* 980.8 as observed for the native enzyme appeared (Fig. 2B). These results indicate that one or two ^{18}O atoms are introduced into the enzyme during incubation with the substrate fluoroacetate in $H_2{}^{18}O$.

Tandem MS/MS Analysis of the ^{18}O-Labeled Peptide—The amino acid residue labeled with ^{18}O of the octapeptide was determined by tandem MS/MS spectrometry. The parent ions of *m/z* 984.8 and 980.8 corresponding to the ^{18}O-labeled and unlabeled octapeptide, respectively, were selected in the first quadrupole and subjected to collision-induced fragmentation in the second quadrupole. The daughter ions produced are shown in Fig. 3. The Y series ions at *m/z* 700.7, 587.5, 488.3, 431.4, and 294.3 derived from the ^{18}O-labeled octapeptide were assigned as the fragment ions due to Leu–Val–Gly–His–Asp–Arg, Val–Gly–His–Asp–Arg, Gly–His–Asp–Arg, His–Asp–Arg, and Asp–Arg, respectively (Fig. 3A). These ions are about 4 Da higher than those derived from the unlabeled peptide at *m/z* 696.6, 583.5, 484.4, 427.4, and 290.0, respectively (Fig. 3B). However, the molecular mass of the fragment ion for the C-terminal Arg derived from the labeled peptide (*m/z* 175.0) was similar to that from the unlabeled peptide (*m/z* 175.1). These results indicate that both of the two ^{18}O atoms occur at Asp next to the Arg: the carboxyl group of Asp-105 is labeled with ^{18}O

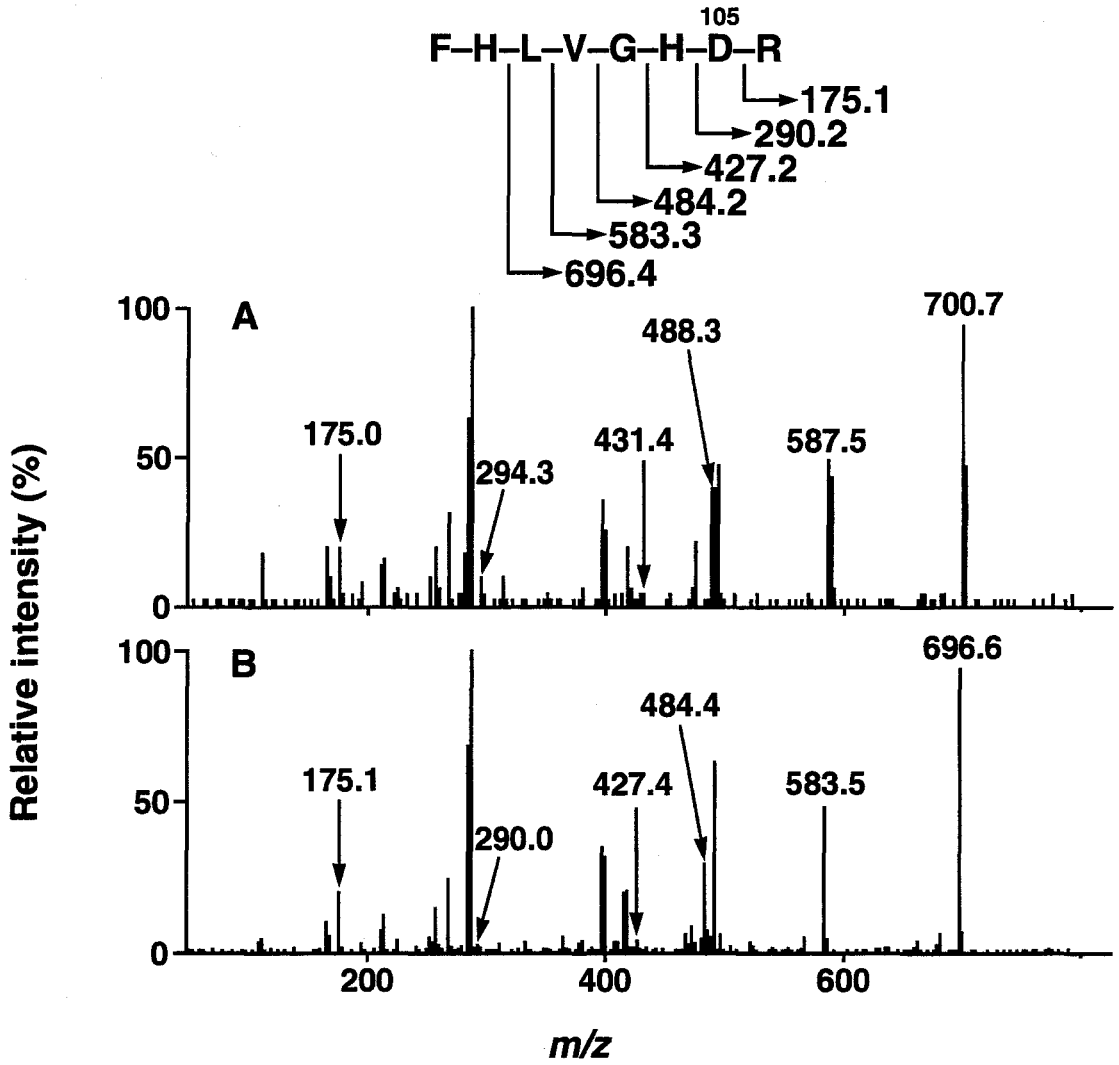

FIG. 3. **Tandem MS/MS daughter ion spectra of ^{18}O-labeled and unlabeled octapeptides Phe-99–Arg-106.** The calculated value of each peptide fragment is indicated in the sequence of the peptide. The fragment ions produced from the ^{18}O-labeled peptide (A) and those from the unlabeled peptide (B) are shown.

atoms during the enzymatic dehalogenation in $H_2{}^{18}O$.

Labeling of H272N with [^{14}C]Chloroacetate—H272N was incubated with [1-^{14}C]chloroacetate and then deionized by C_{18} reverse phase HPLC. H272N was clearly labeled with chloroacetate (2,710 dpm), whereas only a little radioactivity at a background level (65 dpm) was incorporated into the wild-type enzyme. His-272 probably plays an essential role in the hydrolysis of the alkylated enzyme derived from the substrate, and H272N provided the alkylated enzyme upon incubation with the substrate.

MS Analysis of the Labeled Peptide Derived from H272N—It was examined by ion-spray mass spectrometry whether H272N is also modified with fluoroacetate. The molecular mass of H272N incubated with fluoroacetate was 33,316 Da, which is 58 Da higher than that of the unreacted mutant enzyme (33,258 Da). The molecular mass of the deprotonated form of carboxymethylene moiety of fluoroacetate is 58 Da. Therefore, the mutant enzyme is probably modified by the carboxymethylene moiety of fluoroacetate.

The modified H272N was digested with trypsin, and the resultant peptide fragments were analyzed by ion-spray mass spectrometry. When the spectrometer was in the single-quadrupole mode, the total ion current chromatogram displayed several peaks (Fig. 4). Peak A contained an $[M + H]^+$ ion at *m/z* 980.6; Peak B contained an $[M + H]^+$ ion at *m/z* 1038.6. They are probably the unmodified and modified octapeptide Phe-99–Arg-106, and were derived from the unmodified and modified enzyme, respectively. The other peaks were those derived from other regions of the enzyme (data not shown). The difference in mass between Peaks A and B (58 Da) agrees well with the calculated mass of the carboxymethylene moiety of fluoroacetate (Fig. 4). Although the modified residue of the octapeptide was not determined by tandem MS/MS analysis, Asp-105 is the most probable candidate for the site of modification because it was specifically labeled with ^{18}O in $H_2{}^{18}O$ as described above. The carboxylate anion of Asp-105 probably acts as a nucleophile to attack the α-carbon of fluoroacetate with the release of fluoride anion in an S_N2-type reaction. The putative ester intermediate formed is hydrolyzed by an activated water molecule in the wild-type enzyme. However, H272N is probably unable to activate a water molecule, and the ester intermediate accumulates. In conclusion, the reaction catalyzed by FAc-DEX proceeds through the mechanism shown in Scheme 3: Asp-105 of the enzyme acts as the nucleophile to attack the α-carbon of haloacetate to form an ester intermediate, which is then hydrolyzed by a water molecule activated by His-272.

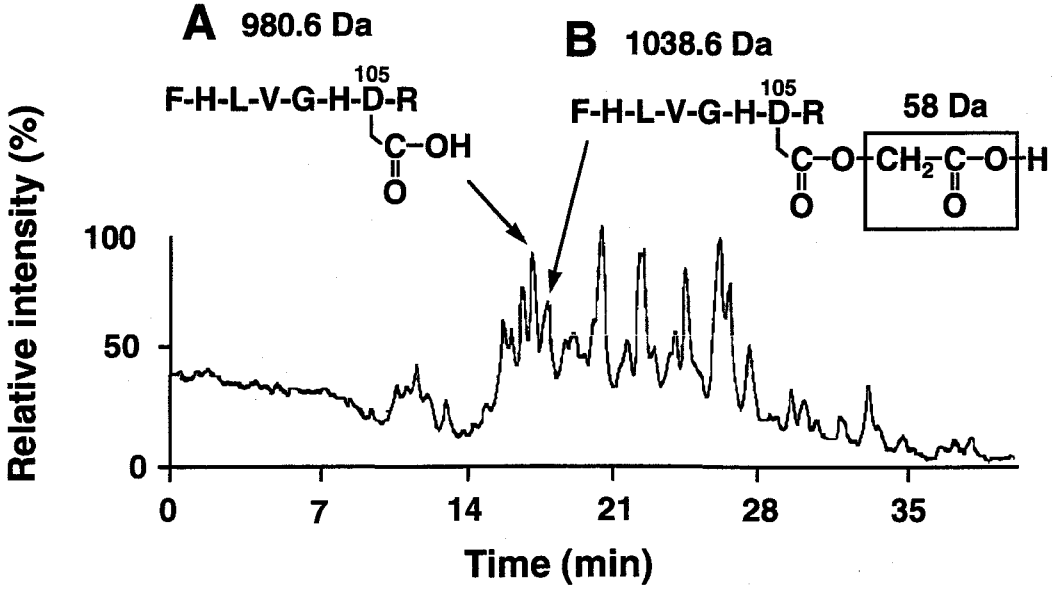

FIG. 4. **Reverse phase HPLC elution profile of proteolytic fragments of H272N incubated with fluoroacetate.** The structure of the unmodified octapeptide Phe-99–Arg-106 (A) and a possible structure of the modified octapeptide Phe-99–Arg-106 (B) are shown.

Scheme 3. **Proposed reaction mechanism of FAc-DEX.**

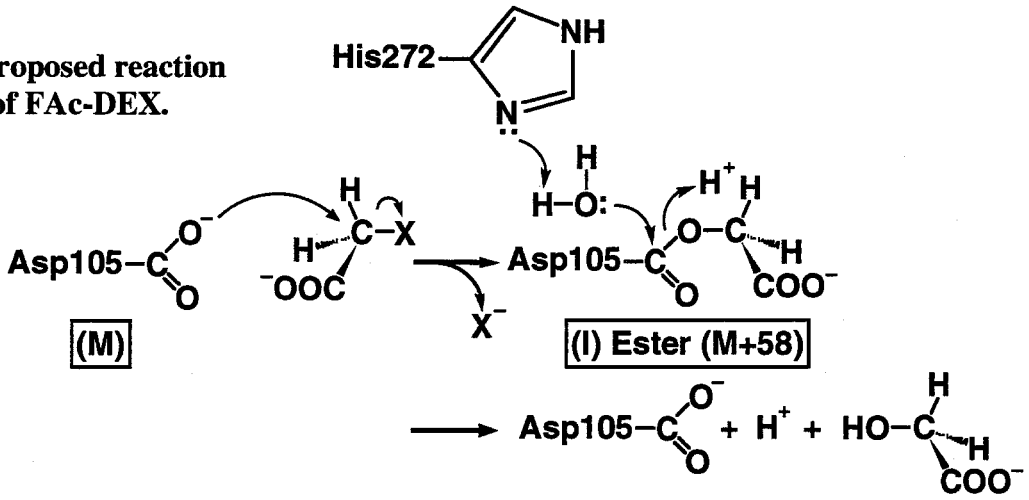

Mass Spectrometric Analysis of FAc-DEX Incubated with Fluoroacetate in H_2O or D_2O—Structural change of FAc-DEX in the course of the catalytic reaction can be monitored by ion-spray mass spectrometry as shown in Fig. 5. The control enzyme not incubated with fluoroacetate showed a peak at 33,281 Da (M), which is identical to the value predicted from the nucleotide sequence. After 4 sec of the incubation in H_2O, the M peak decreased, and a new peak at 33,339 Da (M+58) appeared, which is

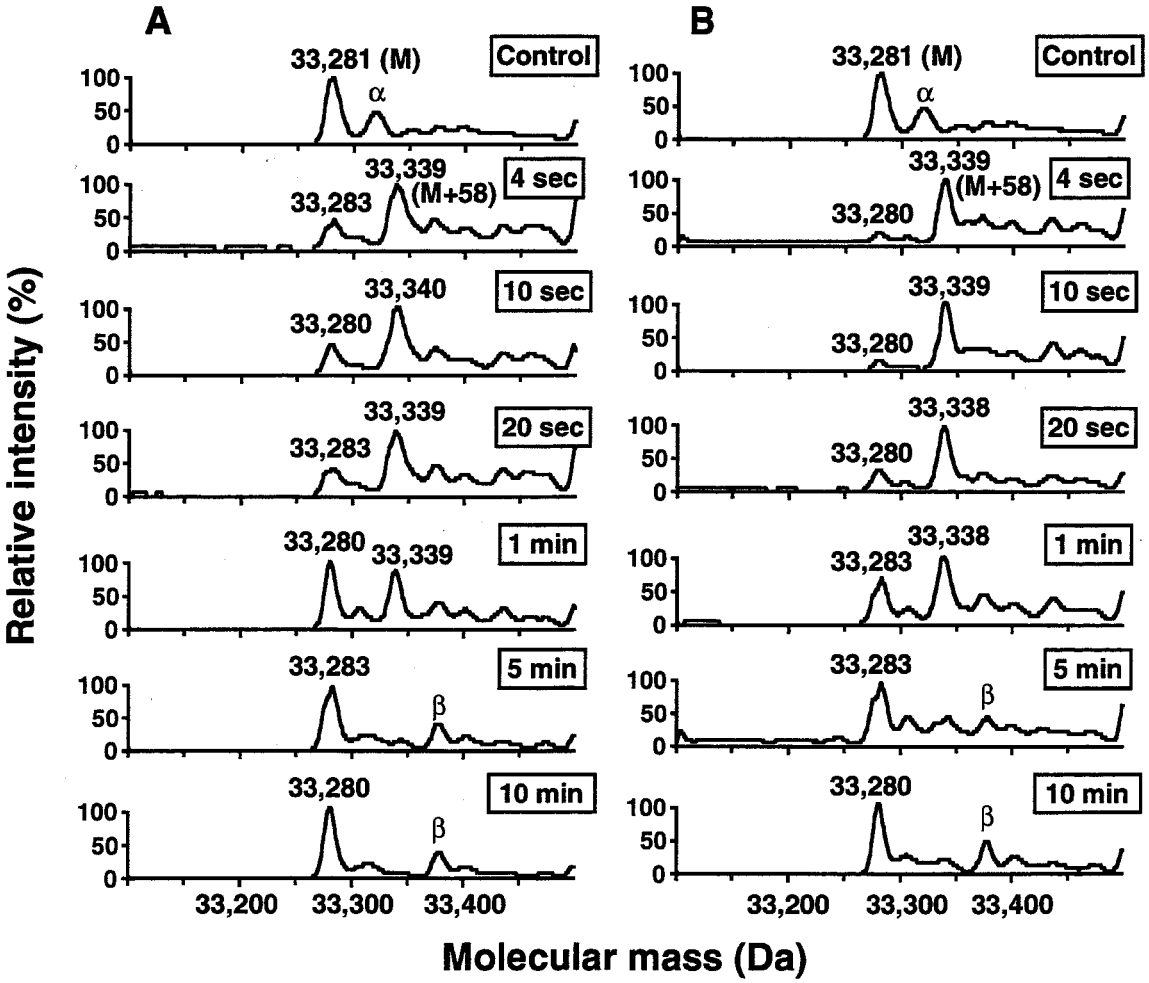

FIG. 5. **Structural changes of FAc-DEX incubated with fluoroacetate in H_2O (A) and D_2O (B).** FAc-DEX was incubated with fluoroacetate in H_2O (A) or in D_2O (B) for indicated times, denatured by addition of formic acid, deionized by HPLC, and analyzed by ion-spray mass spectrometry. An error of ± 3 Da is acceptable in analysis of a protein around 33 kDa with the mass spectrometer used. Peak α can be assigned as the enzyme with a potassium ion (33,320 Da); Peak β, the enzyme with a sulfate ion (33,378 Da).

considered to be the enzyme forming an ester intermediate (I, M+58) as shown in Scheme 3 (Fig. 5A). The enzyme occurred predominantly as the M+58 variant from 4 to 20 sec, indicating that the rate-limiting step of the FAc-DEX reaction is hydrolysis of the ester intermediate. The population corresponding to the original peak (M) increased over a period from 10 sec to 1 min and became predominant, as the M+58 peak decreased and disappeared. This is probably due to the substrate exhaustion by the enzyme reaction.

If hydrolysis of the ester intermediate is the rate-limiting step as suggested in the above experiment, the ratio of the M+58 variant to the M variant is expected to increase when the enzyme reaction was carried out in D_2O because the dissociation energy of an O–D bond is higher than that of an O–H bond. When the enzyme reaction was carried out in D_2O, mass spectral change of FAc-DEX occurred as shown in Fig. 5B. In contrast to Fig. 5A, the M peak almost disappeared over a period from 4 to 10 sec. Judging from the peak height ratio at 10 sec, the M+58 population formed upon incubation in H_2O accounts for about 69% of the whole enzyme molecules, whereas the M+58 population accounts for about 88% when incubated in D_2O. This result indicates that the ester intermediate is present more abundantly in D_2O than in H_2O, supporting the view that the hydrolysis of the ester intermediate is the rate-limiting step of the reaction.

DISCUSSION

FAc-DEX has an amino acid sequence with a limited but significant similarity to that of DhlA (Fig. 1, p.11). Both enzymes are members of the same family of α/β hydrolases (19) and contain aspartate and histidine as catalytic residues conserved in all members. I have proposed that the FAc-DEX enzyme reaction proceeds through the mechanism as follows: Asp-105 acts as a nucleophile which substitutes for a halogen atom in the substrate, and the ester intermediate formed is then hydrolyzed by a water molecule activated by His-272. A similar mechanism has been proposed for the reaction catalyzed by DhlA. The substrate specificities of the two dehalogenases, however, are quite different from each other: DhlA catalyzes the hydrolysis of chlorinated and brominated *n*-alkanes, and FAc-DEX catalyzes the dehalogenation of fluoroacetate and other haloacetates. Both dehalogenases probably originated from a common ancestor protein, but have diverged by evolution to the present enzymes with different substrate specificities.

Phe-128 of DhlA serves as a binding site for the Cl-2 atom, which is not dechlorinated, of the substrate 1,2-dichloroethane (26). The amino acid sequence around this residue is conserved in FAc-DEX, and the residue is replaced by Arg-109 in the latter enzyme (Fig. 1, p.11). Arginine is the most common binding site of various enzymes for the carboxyl group of substrates. Therefore, Arg-109 of the fluoroacetate dehalogenase probably acts as the binding site for the carboxyl group of haloacetates.

The halogen-binding sites of various enzymes have been clarified by X-ray

crystallography: His-197 and Lys-200 of human color vision pigments for chloride ion (49); Thr-199 of carbonic anhydrase II for bromide ion (50); Arg-337, Arg-195, and Asn-298 of pig pancreatic α-amylase for chloride ion (51). Trp-125 and Trp-175 of DhlA serve as the binding site of the Cl-1 atom, which is dechlorinated, of 1,2-dichloroethane (26). They are conserved as Arg-106 and Trp-151 in FAc-DEX, respectively (Fig. 1, p.11), suggesting that they possibly function as the binding site for the fluorine atom of fluoroacetate. In fact, replacement of Arg-106 of FAc-DEX by Gly, Lys, Ser, and even Trp, the last of which yields the mutant enzyme imitating the halogen binding site of DhlA, resulted in total inactivation. Similarly, Kennes et al. have replaced Trp-125 of DhlA with Arg in order to mimic the putative halogen-binding site of FAc-DEX, and reported that the resulting enzyme showed no activity on either 1,2-dibromo- or 1,2-dichloroethane (28). The halogen binding site of FAc-DEX is probably constructed by a complicated network with various polar and charged amino acid residues around Arg-106.

In Australia, rumen bacteria genetically modified to express recombinant FAc-DEX have been applied to the detoxification of poisonous plants containing high concentrations of fluoroacetate to prepare for cases in which these plants are ingested by domestic animals (52). FAc-DEX can possibly be engineered through protein engineering to change its activity, making it capable of decomposing various fluorocompounds other than fluoroacetate such as flons which have caused environmental problems.

SUMMARY

FAc-DEX catalyzes the dehalogenation of fluoroacetate and other haloacetates. The amino acid sequence of FAc-DEX is similar to that of DhlA in the regions around Asp-105 and His-272, which correspond to the active site nucleophile Asp-124 and the base catalyst His-289 of DhlA, respectively. After multiple turnovers of the FAc-DEX reaction in $H_2{}^{18}O$, the enzyme was digested with trypsin, and the molecular masses of the peptide fragments formed were measured by ion-spray mass spectrometry. Two ^{18}O atoms were shown to be incorporated into the octapeptide, Phe-99–Arg-106. Tandem mass spectrometric analysis of this peptide revealed that Asp-105 was labeled with two ^{18}O atoms. These results indicate that Asp-105 acts as a nucleophile to attack the α-carbon of the substrate, leading to the formation of an ester intermediate, which is subsequently hydrolyzed by the nucleophilic attack of a water molecule on the carbonyl carbon atom. The H272N mutant enzyme showed no activity with either fluoroacetate or chloroacetate. However, ion-spray mass spectrometry revealed that H272N was covalently alkylated with the substrate. The reaction of H272N with [^{14}C]chloroacetate also showed the incorporation of radioactivity into the enzyme. These results suggest that His-272 acts as a base catalyst for the hydrolysis of the covalent ester intermediate.

CHAPTER II

Paracatalytic Modification of the Nucleophile Asp-105 of Fluoroacetate Dehalogenase by Hydroxylamine and Ammonia

INTRODUCTION

Paracatalytic enzyme inactivation is a catalysis-linked and substrate-dependent enzyme inactivation. It involves a direct chemical reaction between an enzyme-activated substrate and an extrinsic reagent which is not a constituent of the normal enzyme–substrate system, causing irreversible covalent modification of an active site of the enzyme (53, 54).

FAc-DEX catalyzes the hydrolytic dehalogenation of fluoroacetate and other haloacetates to produce glycolate as described in Chapter I. I have proposed that the enzyme reaction proceeds through the mechanism shown in Scheme 3 (p.15): Asp-105 acts as a nucleophile causing the release of a halide ion and the formation of an ester intermediate, which is subsequently hydrolyzed by a water molecule activated by His-272. The reactions catalyzed by other hydrolases, such as L-DEX YL (16, 20) and DhlA (22, 26, 27), also proceed through similar mechanisms involving the formation of an enzyme–substrate ester intermediate.

Hydroxylamine is a strong nucleophilic reagent. It has been used as an inhibitor of enzymes containing pyridoxal 5'-phosphate, such as aspartate aminotransferase (55). Hydroxylamine has also been used successfully as an acyl group acceptor to trap acyl–enzyme intermediates. Shao et al. used hydroxylamine to show ester intermediate formation in protein splicing (56). Ammonia can react with an ester intermediate in the same manner as hydroxylamine; thus Howard et al. used ammonia to cleave the ester linkage formed between a labeling reagent and the catalytic nucleophilic residue of jack bean α-mannosidase (57). Therefore, either hydroxylamine or ammonia possibly serves as a nucleophile to demonstrate ester-intermediate formation in FAc-DEX reaction.

The active site Asp-10 of L-DEX YL was shown to be specifically modified by hydroxylamine in the presence of L-2-haloalkanoic acid to produce either aspartate β-hydroximate carboxyalkyl ester residue (Scheme 4, Passway 2, IV) or aspartate β-hydroxamic acid residue (Scheme 4, Passway 1, III), where IV was the major product (17). In this study, I demonstrate that the active site Asp-105 of FAc-DEX is paracatalytically modified with hydroxylamine in the same manner. However, FAc-DEX differs markedly from L-DEX YL: aspartate β-hydroxamic acid (III) was the only product in the paracatalytic modification of FAc-DEX. I also report here that Asp-105 of FAc-DEX is paracatalytically converted to asparagine in the presence of ammonia (Scheme 5).

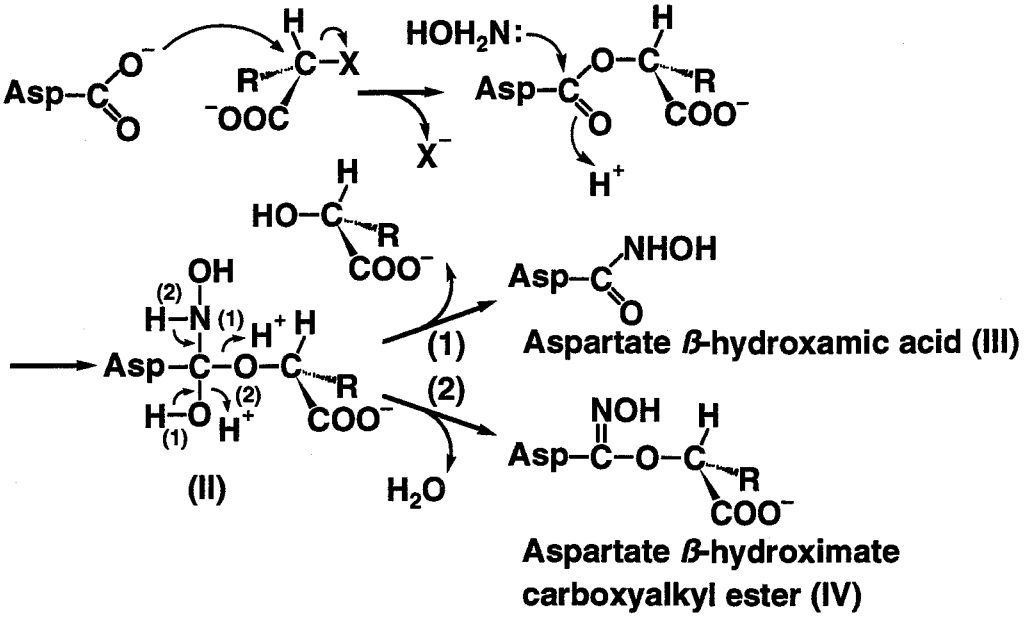

Scheme 4. **Probable mechanisms of paracatalytic inactivation of FAc-DEX and L-DEX YL by hydroxylamine.**

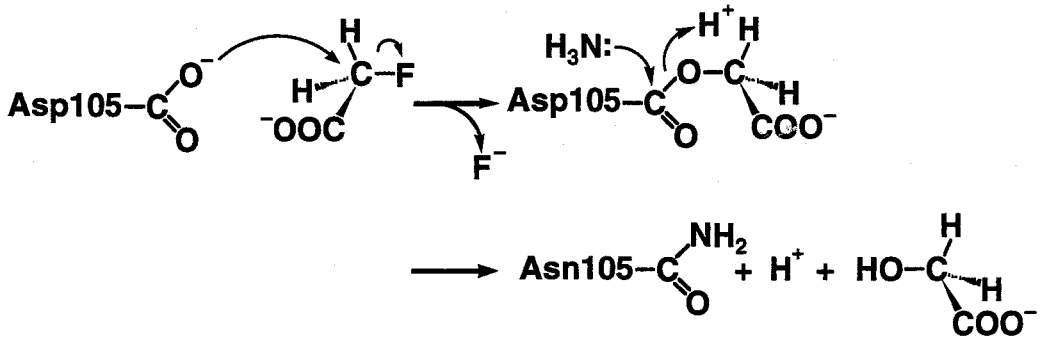

Scheme 5. **Paracatalytic inactivation of FAc-DEX by ammonia.**

EXPERIMENTAL PROCEDURES

Materials—Hydroxylamine sulfate, and protamine sulfate were purchased from Wako Pure Chemical Industries (Osaka, Japan), ammonia solution (28%) and ammonium sulfate from Nacalai Tesque (Kyoto, Japan), Butyl-Toyopearl from Tosoh (Tokyo), and *N*-tosyl-L-phenylalanyl chloromethyl ketone(TPCK)-treated trypsin from Sigma (St. Louis, MO). All other chemicals were of analytical grade.

Enzyme Purification—The purification procedure for FAc-DEX was slightly modified from that described in "Experimental Procedures" of Chapter I. The recombinant *E. coli* cells producing the enzyme were grown, harvested, and disrupted by sonication. DNA and its binding proteins were removed from the supernatant with 0.2% protamine sulfate. The supernatant was fractionated with ammonium sulfate. A fraction of 40–70% saturation was dissolved in the standard buffer, and then applied to a Butyl-Toyopearl 650 column (3 × 25 cm). The column was washed with 500 ml of the buffer supplemented with 30% (w/v) ammonium sulfate, and the enzyme was eluted with a linear gradient of 30–0% ammonium sulfate in the buffer with a total

volume of 1 liter. The active fractions, dialyzed against 10 mM potassium phosphate (pH 7.5), were applied to the DEAE-Toyopearl 650M column (1.7 × 5 cm) equilibrated with the same buffer. The enzyme was eluted with a linear gradient of 10–50 mM potassium phosphate (pH 7.5). The active fractions were pooled and used as a purified preparation of the enzyme, which had a specific activity of 13 units/mg. The total yield of the enzyme in the purification was about 39%.

Determination of the Enzyme Activity—FAc-DEX was routinely assayed by determination of chloride ions produced from chloroacetate by the method of Iwasaki et al. (47). The dehalogenation reaction was carried out as described in Chapter I.

Inactivation of FAc-DEX by Hydroxylamine and Ammonia—The reaction was carried out at 30°C in 500 µl of a mixture containing 15 nmol of the enzyme, 75 µmol of Tris-sulfate (pH 9.0), 900 µmol of sodium hydroxide, 50 µmol of sodium fluoroacetate, and 500 µmol of hydroxylamine sulfate. After 1 h, 50 µmol of sodium fluoroacetate was added, and the mixture was incubated for another 1 h. The reaction with ammonia was carried out in the same manner as with hydroxylamine, with the exceptions that 500 µmol of ammonium sulfate was used in place of hydroxylamine sulfate, and sodium hydroxide was omitted. The reaction mixture was dialyzed against 8×10^6 volumes of the standard buffer for 14 h, and then the residual enzyme activities were measured by the method described above (Chapter I). Fluoroacetate or hydroxylamine (or ammonia) was omitted in a control experiment.

Digestion of FAc-DEX with Trypsin—The enzyme inactivated and dialyzed as described above was lyophilized, dissolved in 100 µl of 8 M urea in 200 mM Tris-sulfate buffer (pH 7.2), and incubated at 37°C for 1 h. The enzyme was then digested by addition of 7.5 µg of TPCK-treated trypsin dissolved in 400 µl of 120 mM Tris-sulfate buffer (pH 7.5) at 37°C for 12 h.

LC/MS Analysis of the Peptides Containing Asp-105—The proteolysates (20 µl) described above were mixed with 1 µl of 20% (v/v) 2-mercaptoethanol, incubated for 1 h, and loaded onto a C_{18} reverse phase HPLC column (Michrom BioResources 5 µ 100 Å, 1.0 × 150 mm) connected to a mass spectrometer, PE-Sciex API 300, equipped with an ion-spray ion source. Elution was carried out with 2% acetonitrile containing 0.1% formic acid for 5 min, followed by a linear gradient of 2–62% acetonitrile containing 0.1% formic acid over 60 min at a flow rate of 40 µl/min. The total ion current chromatogram was recorded in the single-quadrupole mode. The quadrupole was scanned from 300 to 2,000 amu with a step size of 0.2 amu and with a dwell time of 0.5 ms/step. The ion-spray voltage was set at 5 kV, and the orifice potential was 30 V. The molecular mass of each peptide was calculated using a Bio-MultiView software supplied by PE-Sciex.

LC/MS/MS Analysis of the Peptides Containing Asp-105—The proteolysates were applied to the HPLC column connected to the mass spectrometer and eluted in the same manner as described above. The daughter ion spectra were obtained in the

triple-quadrupole daughter ion scan mode by introducing the peptides containing Asp-105 ($[M + 2H]^{2+}$ at *m/z* 498.4, 491.0, or 490.4) from Q1 into a collision cell (Q2) and observing the daughter ions in Q3. Q1 was locked on *m/z* 498.4, 491.0, or 490.4. Q3 was scanned from 30 to 1,000 amu with a step size of 0.2 amu and with a dwell time of 0.5 ms/step. The ion-spray voltage was set at 4.8 kV, and the orifice potential was 30 V.

Molecular Modeling of FAc-DEX—The structure of FAc-DEX was predicted by homology modeling on the basis of the structures of DhlA (26, 48) and bromoperoxidase A2 from *Streptomyces aureofaciens* (BpoA2) (58) by using the program MODELLER, version 4 (59). The PHD secondary structure prediction (60) was used to make structure-based sequence alignments. Complete optimization cycles were carried out by means of conjugate gradients and simulated annealing. Five models were generated for the enzyme. The quality of these structures were examined by PROCHECK (61) and by using Protein Health and 3D profile (62) modules of Quanta. All other estimations of structural parameters were carried out using the software Quanta 4.0 or Insight2 (Molecular Simulations, Burlington, MA). The calculations were performed on a Silicon Graphics Indigo2 workstation.

RESULTS

Inactivation of FAc-DEX by Hydroxylamine and Ammonia—FAc-DEX was inactivated significantly upon incubation with fluoroacetate and either hydroxylamine or ammonia, but that omission of fluoroacetate caused no significant inactivation of the enzyme (Fig. 6). The enzyme activity was not restored by extensive dialysis of the

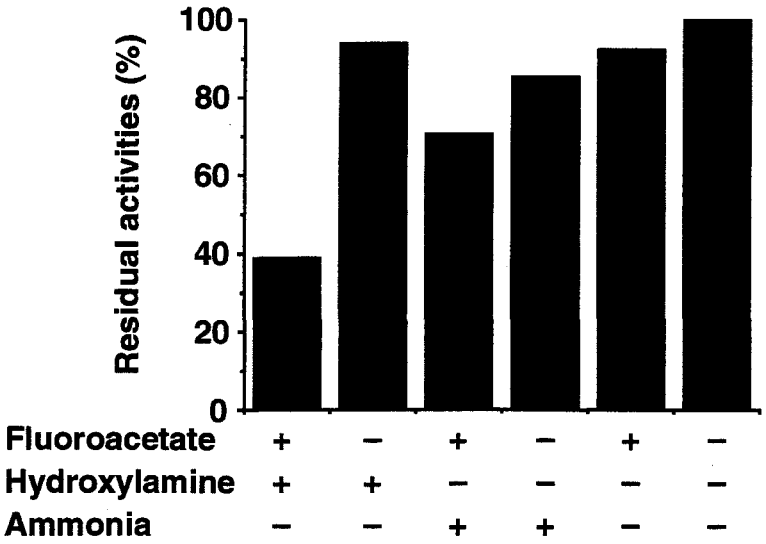

FIG. 6. **Effect of hydroxylamine and ammonia on the FAc-DEX activity.** The enzyme was incubated in the absence (-) or presence (+) of hydroxylamine, ammonia, and substrate fluoroacetate, and its residual activities were measured as described in "Experimental Procedures."

inactivated enzyme, indicating that the inactivation was due to a covalent modification of the enzyme.

Determination of Molecular Mass of the Proteolytic Peptides Modified by Hydroxylamine in the Presence of Fluoroacetate—FAc-DEX inactivated with hydroxylamine was digested with TPCK-treated trypsin, and the resultant peptide fragments were separated by HPLC and analyzed by ion-spray mass spectrometry. When the spectrometer was in the single-quadrupole mode, the total ion current chromatogram displayed several peaks: one of them was assigned to a derivative of the octapeptide Phe-99–Arg-106 (data not shown). The ion-spray mass spectrum of the octapeptide showed two peaks at *m/z* 995.8 and 498.4, which were assigned to $[M + H]^+$ and $[M + 2H]^{2+}$ ions, respectively (Fig. 7A). However, when fluoroacetate was omitted from the reaction mixture, two peaks were observed at *m/z* 980.6 and 491.0, corresponding to $[M + H]^+$ and $[M + 2H]^{2+}$ ions, respectively (Fig. 7B). These peaks probably correspond to unmodified octapeptide Phe-99–Arg-106. Thus, I have found that a carboxylate side chain of an amino acid residue in the peptide was converted to a hydroxamic acid only when the enzyme was incubated with both hydroxylamine and fluoroacetate. Asp-105, being the only acidic residue in the octapeptide, is the most probable candidate for the modified residue.

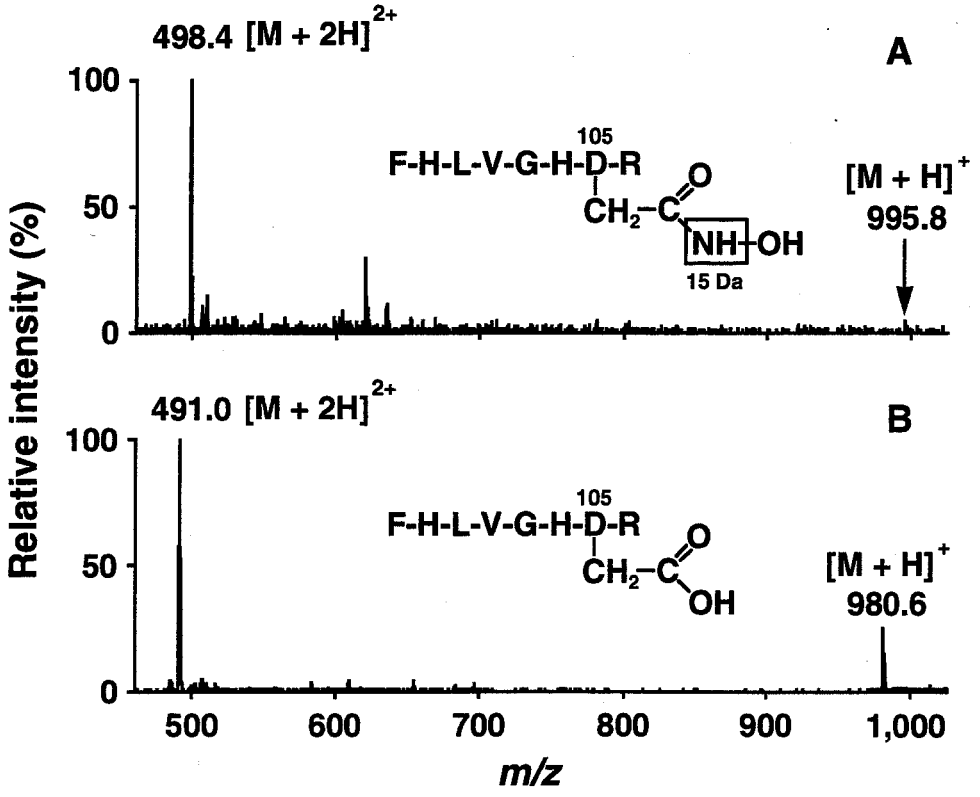

FIG. 7. **LC/MS analysis of proteolytic fragments of FAc-DEX inactivated by hydroxylamine in the presence of fluoroacetate.** Ion-spray mass spectra of the octapeptides Phe-99–Arg-106 derived from the enzyme incubated with (A) or without (B) fluoroacetate in the presence of hydroxylamine. The structure of the unmodified peptide (B) and a possible structure of the modified peptide (A) are shown.

LC/MS/MS Analysis of the Peptide Modified with Hydroxylamine—The amino acid residue modified with hydroxylamine was determined by tandem LC/MS/MS analysis. The parent ions of $[M + 2H]^{2+}$ at *m/z* 498.4 and 491.0 corresponding to the modified and unmodified octapeptides, respectively, were selected in the first quadrupole, and subjected to the collision-induced fragmentation in the second quadrupole. The daughter ions are shown in Fig. 8. The Y series ions ($[M + H]^{+}$) at *m/z* 711.2, 598.2, 499.0, 442.4, and 304.8 in Fig. 8B were considered to be modified derivatives of Leu–Val–Gly–His–Asp–Arg, Val–Gly–His–Asp–Arg, Gly–His–Asp–Arg, His–Asp–Arg, and Asp–Arg, respectively. These ions were about 15 Da higher than those derived from the unmodified peptide at *m/z* 696.4, 583.2, 484.4, 427.4, and 290.0, respectively (Fig. 8A). However, the molecular mass of the fragment ion for the C-terminal Arg derived from the modified peptide was identical to that from the unmodified peptide (*m/z* 175.0). These results indicate that the modification causing 15-Da increase occurs at the position next to the C-terminal Arg, which is Asp-105. The carboxyl group of Asp-105 is probably converted to hydroxamic acid while the enzyme catalyzes dehalogenation of fluoroacetate in the presence of hydroxylamine.

Determination of Molecular Mass of the Proteolytic Peptides Modified by Ammonia in the Presence of Fluoroacetate—FAc-DEX incubated with ammonia in the presence of fluoroacetate was digested, and the resultant peptide fragments were separated and analyzed in the same manner as described above. The total ion current chromatogram displayed several peaks: two of them (Peaks 1 and 2) were assigned to modified and unmodified octapeptide Phe-99–Arg-106, respectively (Fig. 9A). Peak 2 provided an ion-spray mass spectrum (Fig. 9C) virtually identical to that shown in Fig. 7B: Peak 2 is the unmodified peptide. However, Peak 1 provided two ions at *m/z* 979.6 and 490.4 (Fig. 9B), which were 1.2 and 0.6 *m/z* units lower than those of the corresponding ions from Peak 2, and assigned to $[M + H]^{+}$ and $[M + 2H]^{2+}$ ions, respectively. Therefore, Peak 1 contains a derivative of the octapeptide modified with ammonia. The carboxyl group of Asp-105 was most probably modified to an amide group.

LC/MS/MS Analysis of the Peptide Modified with Ammonia—The ions of $[M + 2H]^{2+}$ at *m/z* 490.4 and 491.0 corresponding to the modified and unmodified octapeptides, respectively, were analyzed further by tandem LC/MS/MS (Fig. 8C). The Y series monovalent ions at *m/z* 695.4, 582.2, 483.2, 426.0, and 289.0 derived from the parent divalent ion at *m/z* 490.4 were assigned to derivatives of Leu–Val–Gly–His–Asp–Arg, Val–Gly–His–Asp–Arg, Gly–His–Asp–Arg, His–Asp–Arg, and Asp–Arg, respectively (Fig. 8C). They were about 1 Da lower than those derived from the unmodified peptide at *m/z* 696.4, 583.2, 484.4, 427.4, and 290.0, respectively (Fig. 8A). However, the molecular mass of the fragment ion for the C-terminal Arg derived from the modified peptide (*m/z* 175.2) was virtually identical to

that from the unmodified peptide (*m/z* 175.0). These results indicate that Asp-105 adjacent to the C-terminal Arg was specifically modified in such a way as its molecular mass becomes 1 Da lower than the original value: the carboxyl group of Asp-105 was most probably converted to the amide.

Determination of Asparagine Residue by Protein Sequencing—The modified peptide (Peak 1 in Fig. 9A) was isolated by HPLC with the C_{18} reverse phase HPLC column (Millipore Puresil 5 μ C_{18} 120 Å, 4.6 × 150 mm), and sequenced with the

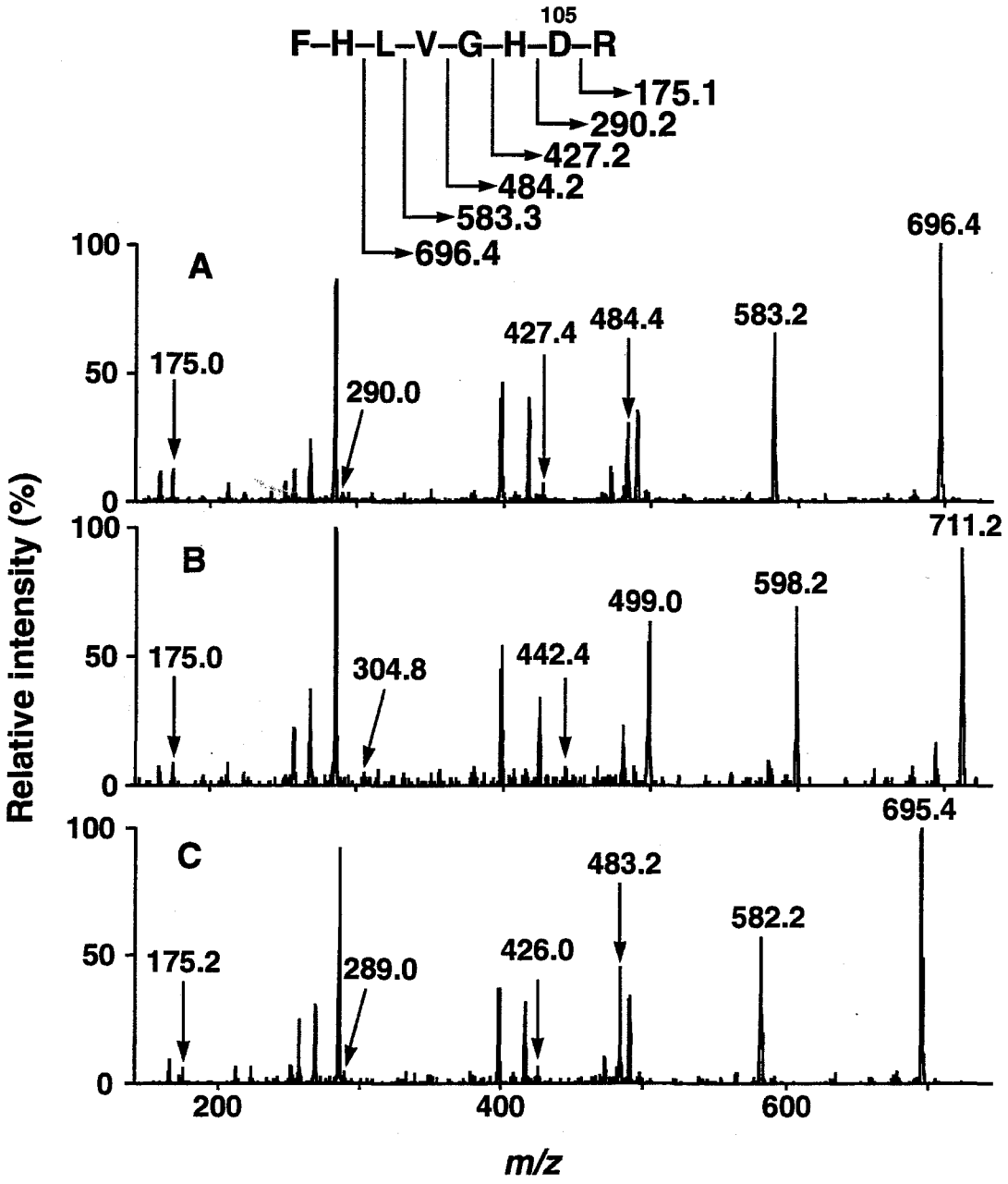

FIG. 8. **Tandem LC/MS/MS daughter ion spectra of the octapeptides Phe-99–Arg-106 from unmodified and modified FAc-DEX.** The calculated *m/z* values of fragment ions produced from the unmodified peptide are indicated. The MS/MS spectra of the unmodified peptide (A) and the modified peptide with hydroxylamine (B) were measured with the precursor ions of $[M + 2H]^{2+}$ at *m/z* 491.0 and 498.4, respectively. The spectrum of the peptide modified with ammonia (C) was obtained with the precursor ion $[M + 2H]^{2+}$ at *m/z* 490.4. The mass values of only monovalent ions are indicated.

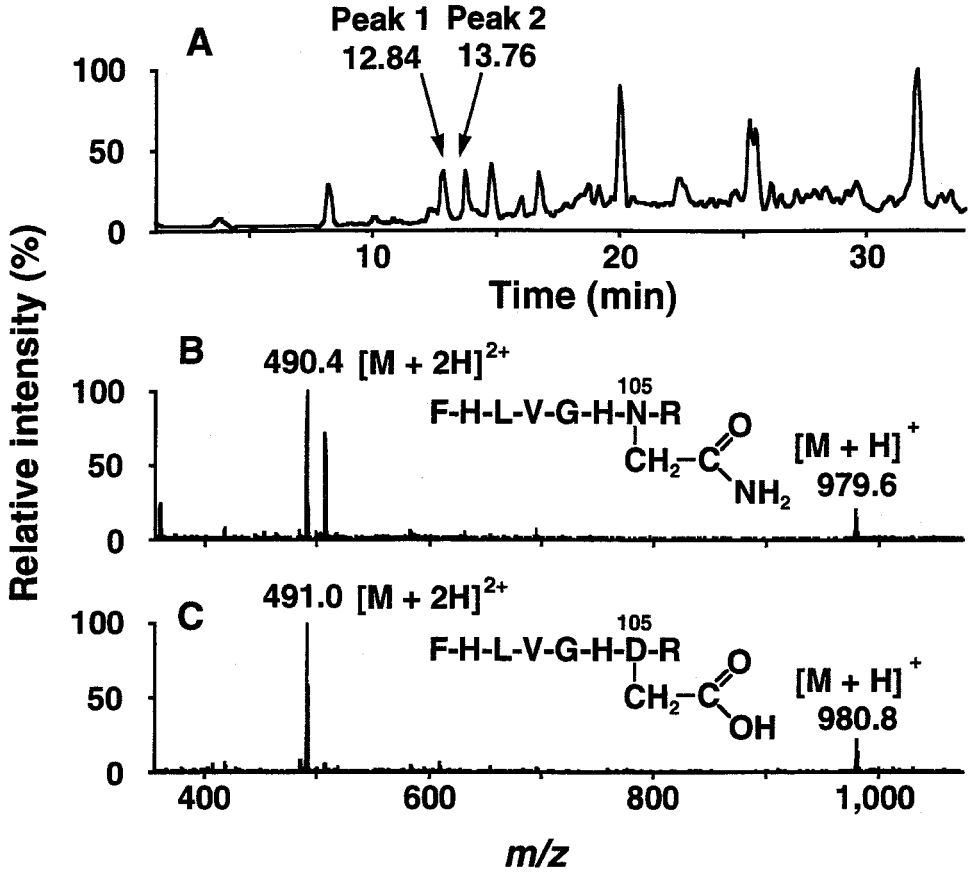

FIG. 9. **LC/MS analysis of the proteolytic fragments of FAc-DEX inactivated by ammonia in the presence of fluoroacetate.** *A*, total ion current chromatogram of proteolytic fragments; *B* and *C*, ion-spray mass spectra of the peptides containing Asp-105 of Peaks 1 and 2 shown in *A*, respectively. Possible structures of these peptides are also shown.

Shimadzu protein sequencer. A sequence of Phe–His–Leu–Val–Gly–His–Asn–Arg was obtained; with the exception of Asn, this sequence was identical to that predicted from the nucleotide sequence. This indicates that Asp-105 was converted to asparagine by the paracatalytic modification with ammonia.

DISCUSSION

On the basis of ^{18}O-labeling experiments, I have proposed that the FAc-DEX reaction proceeds through the following mechanism (Chapter I): Asp-105 at the active site acts as a nucleophile causing the release of a halide ion and the formation of an ester intermediate, which is subsequently hydrolyzed (Scheme 3, p.15). I have shown here that the enzyme is significantly inactivated when it is incubated with hydroxylamine or ammonia in the presence of fluoroacetate, and that the inactivation is accompanied by specific modification of the nucleophile Asp-105: the residue was converted to aspartate β-hydroxamic acid and asparagine with hydroxylamine and ammonia, respectively (Scheme 6). Note that the presence of substrate fluoroacetate was essential for the modifications. These results indicate that hydroxylamine and ammonia are substituted for water in the second step of the reaction, hydrolysis of the

ester intermediate. Thus, Asp-105 was modified with a nucleophile, hydroxylamine or ammonia.

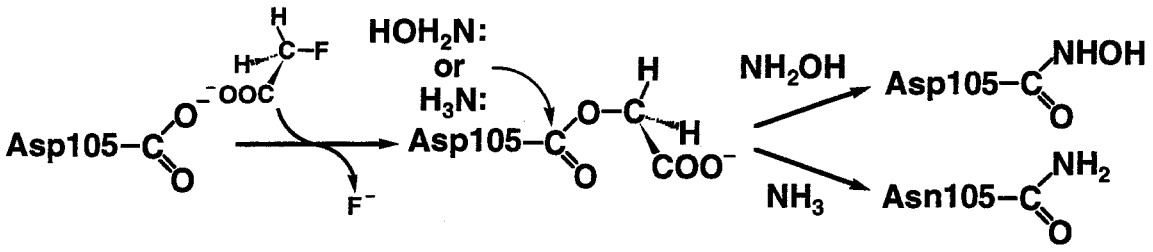

Scheme 6. **Paracatalytic inactivation mechanisms of FAc-DEX by hydroxylamine and ammonia.**

Hydroxylamine has been widely used as a nucleophilic reagent to show formation of an acyl–enzyme intermediate in various hydrolase reactions, such as those involving chymotrypsin (63), D-alanine carboxypeptidase (64), and lipoprotein lipase (65). Production of hydroxamic acid derivatives of normal products provides evidence of the formation of an ester intermediate whose acyl moiety derives from the substrate. In contrast, the acyl moiety of an ester intermediate formed in FAc-DEX reaction originates from the carboxyl group of Asp-105, and the aspartate residue is modified with hydroxylamine. In this study, paracatalytic inactivation with hydroxylamine thus provided a powerful tool for verifying the function of Asp-105 of FAc-DEX.

Recently, L-DEX YL was also shown to be paracatalytically inactivated and modified with hydroxylamine (17): Asp-10, which acts as a nucleophile to attack the α-carbon of L-2-haloalkanoic acids, is converted mainly to aspartate β-hydroximate carboxyalkyl ester residue (Scheme 4, IV, p.20). This provides a clear contrast to the paracatalytic modification of FAc-DEX described above. Compound IV is produced when the β-hydroxyl group of the precursor molecule (Scheme 4, II) is protonated and liberated as a water molecule (Scheme 4, Passway 2). According to the crystal structure of the L-DEX YL S175A mutant enzyme complexed with chloroacetate, Lys-151 is most probably the residue that protonates the β-hydroxyl group of the precursor (20). However, FAc-DEX probably has no relevant residues causing protonation of the β-hydroxyl group, and glycolate, which is regarded as a much better leaving group than the β-hydroxyl group, is liberated to leave aspartate β-hydroxamic acid residue (Scheme 4, Passway 1).

Ion-spray mass spectrometric analyses of L-DEX YL showed that virtually all molecules of the enzyme occur in the ester intermediate form while catalyzing dehalogenation of an L-2-haloalkanoic acid (Chapter IV). However, a significant portion of FAc-DEX molecules (about 40% of the total number) occur in a native form while FAc-DEX catalyzes dehalogenation of a haloacetate (Fig. 5, p.15). These findings indicate that the hydrolysis of the ester intermediate is much slower than the formation of the intermediate in the L-DEX YL reaction. L-DEX YL probably has an

active-site structure suitable for keeping the 2-hydroxyalkanoic acid moiety of the ester intermediate stable, while FAc-DEX probably has no such conditions. This may explain the difference between FAc-DEX and L-DEX YL with respect to the form of aspartate residues paracatalytically modified with hydroxylamine, i.e. Compound III and IV, respectively (Scheme 4, p.20).

Ammonia was also shown to label Asp-105 of FAc-DEX, although ammonia is usually much less nucleophilic than hydroxylamine. In fact, ammonia was inert as a paracatalytic inactivator for L-DEX YL (data not shown). It has been demonstrated that the active site of L-DEX YL is surrounded by a highly hydrophilic environment (18). Therefore, most ammonia molecules occur in the form of ammonium ions, which are inert as nucleophiles, at the active site of this enzyme. In contrast, according to the structure of FAc-DEX built by homology modeling using DhlA and BpoA2 as reference structures (Fig. 10A), the active site of FAc-DEX is characterized by a highly hydrophobic and basic environment (Fig. 10B). It is reasonable to assume that plenty of free ammonia molecules are available at the active site of FAc-DEX.

Hydroxylamine and ammonia probably serve as effective labeling reagents for hydrolytic enzymes whose acidic amino acid residue acts as a nucleophile in the same manner as FAc-DEX.

FIG. 10. **Sequence alignment and molecular modeling of FAc-DEX.** *A*, the sequence alignment of FAc-DEX with DhlA and BpoA2. Predicted secondary structures of FAc-DEX are also shown. *B*, stereoview of the active site model of FAc-DEX (p.29) prepared using program MOLSCRIPT (66). Hydrophobic or basic residues are drawn with thick lines; other types of amino acid residues are drawn with thin lines.

B

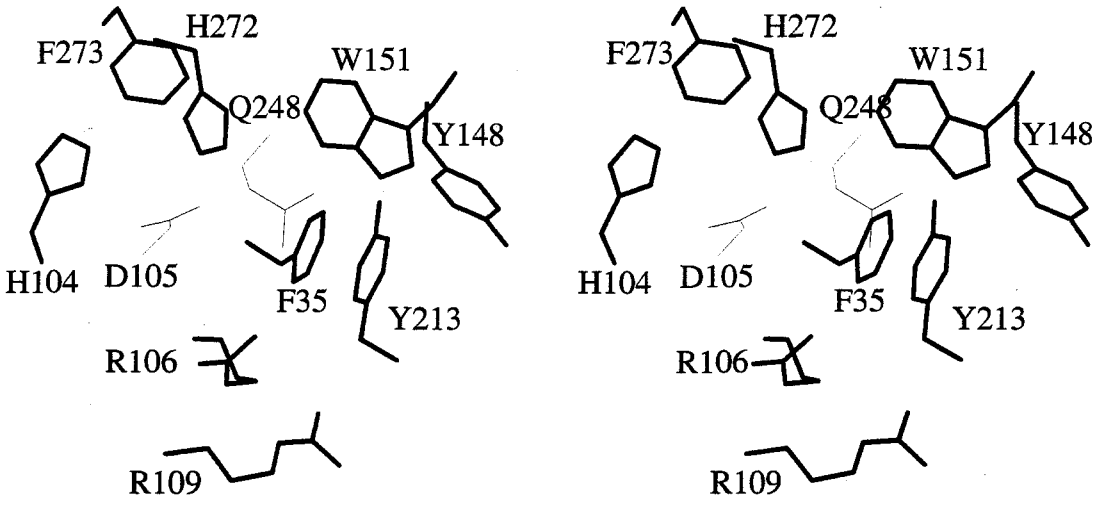
F273
H272
W151
Q248
Y148
H104
D105
F35
Y213
R106
R109
F273
H272
W151
Q248
Y148
H104
D105
F35
Y213
R106
R109

SUMMARY

FAc-DEX catalyzes the hydrolytic dehalogenation of fluoroacetate and other haloacetates. I have proposed that Asp-105 of the enzyme acts as a nucleophile to attack the α-carbon of haloacetate to form an ester intermediate, which is then hydrolyzed by a water molecule activated by His-272 (Chapter I). I have verified my proposal by paracatalytic inactivation studies. I have found that the enzyme is inactivated concomitantly with defluorination of fluoroacetate in the presence of hydroxylamine or ammonia. The enzyme paracatalytically inactivated by these nucleophilic reagents was digested with trypsin, and subjected to ion-spray mass spectrometric analyses. Molecular masses of the peptide fragments containing Asp-105 isolated from the enzyme inactivated by hydroxylamine were shown to be higher by 15 Da than those obtained from the native enzyme. Similarly, the peptides isolated from the enzyme modified with ammonia showed molecular masses 1 Da lower than those from the native enzyme. Tandem mass spectrometric analyses revealed that the modification occurred at Asp-105, indicating that hydroxylamine and ammonia attack the carbonyl carbon atom of the ester intermediate to produce aspartate β-hydroxamic acid and asparagine residues, respectively. The formation of asparagine residue was further confirmed using a gas-phase protein sequencer. These results demonstrate that Asp-105 is the active site residue that attacks the substrate to form an ester intermediate. The results also show hydroxylamine and ammonia to be useful as active-site probes.

CHAPTER III

Hydrolytic Deamidation of Asn-105 of Fluoroacetate Dehalogenase D105N Mutant

INTRODUCTION

FAc-DEX catalyzes the hydrolytic dehalogenation of fluoroacetate and other haloacetates to produce glycolate. I have shown that the enzyme reaction proceeds through the following mechanism: Asp-105 acts as a nucleophile causing the release of a halide ion and the formation of an ester intermediate, which is subsequently hydrolyzed by a water molecule activated by His-272 (Scheme 3, p.15). Replacement of Asp-105 by Ala, Gly, and Val yielded mutant enzymes showing no dehalogenation activity. However, replacement of Asp-105 by Asn did not completely inactivate the enzyme.

The reactions catalyzed by other hydrolases, such as DhlA (22) and MEH (41), both of which show sequence similarity with FAc-DEX, have also been shown to proceed via an ester intermediate: Asp-124 and Asp-226 act as a nucleophile, respectively. Pries et al. have reported that DhlA D124N undergoes autoactivation, in which Asn-124 is spontaneously converted into Asp (67). Laughlin et al. have shown autoactivation of MEH D226N (68). The deamidation of Asn probably occurs by direct attack of a water molecule that acts as a nucleophile in hydrolysis of an ester intermediate in the wild-type enzyme reaction.

I have constructed FAc-DEX D105N mutant enzyme. The mutant enzyme showed a slight dehalogenation activity, and the activity increased during purification and storage. In this chapter, I demonstrate that direct hydrolytic deamidation of Asn-105 causes the generation of the wild-type enzyme, which is responsible for the dehalogenation activity of the mutant enzyme preparation.

EXPERIMENTAL PROCEDURES

Materials—Sequencing grade modified trypsin was purchased from Promega (Madison, WI). All other chemicals were of analytical grade.

Enzyme Preparation—Replacement of amino acid residue was carried out by the method of Kunkel (46). The synthetic mutagenic primer designed for the D105N enzyme was as follows (the underlines indicate the mutagenized nucleotides): 5'-GCGGTTATGTCCGACGA. The substitutions were confirmed with the DNA sequencer. The purification procedure for FAc-DEX D105N was identical to that reported in the "Experimental Procedures" in Chapter II, with the exceptions that protamine sulfate treatment was omitted, and the supernatant fractionated with ammonium sulfate (40% saturation) was immediately applied to the Butyl-Toyopearl 650 column (3 × 25 cm). The fractions containing the mutant enzyme were identified by SDS-PAGE.

Determination of the Enzyme Activity—FAc-DEX was routinely assayed by determination of chloride ions produced from chloroacetate by the method of Iwasaki et al. (47). The dehalogenation reaction was carried out as described in Chapter I.

Digestion of the D105N Enzyme with the Modified Trypsin—D105N (10 nmol) was incubated in the solution (40 µl) containing 4 µmol of Tris-sulfate buffer (pH 9.5). The enzyme was denatured with 0.4 µl of formic acid, dialyzed against deionized water, and lyophilized. The lyophilized enzyme was dissolved in 100 µl of 8 M urea and 5 mM dithiothreitol in 50 mM Tris-chloride buffer (pH 8.5), and incubated at 60°C for 1 h. The enzyme was then digested by addition of 5 µg of the modified trypsin dissolved in 700 µl of 50 mM Tris-chloride buffer (pH 7.6) containing 1 mM calcium chloride at 37°C for 12 h.

LC/MS Analysis of the Peptides Containing Asn-105—The proteolysates were concentrated and loaded onto a C_{18} reverse phase column (Shiseido Capcell Pak, SG 300 Å 5 µm, 4.6 × 250 mm) connected to a mass spectrometer, PE-Sciex API 365 or 3000. Elution was carried out with 2% acetonitrile containing 0.1% formic acid for 5 min, followed by a linear gradient of 2–82% acetonitrile containing 0.1% formic acid over 40 min at a flow rate of 40 µl/min. The total ion current chromatogram was recorded in the single-quadrupole mode. The quadrupole was scanned from 300 to 1,500 amu with a step size of 0.1 amu and with a dwell time of 0.2 ms/step. The ion-spray voltage was set at 5 kV, and the orifice potential was 40 V. The molecular mass of each peptide was calculated using the Bio-MultiView software. For detailed analysis of the peptides containing Asn-105, the HPLC fractions were collected, concentrated, and injected into the mass spectrometer for tandem mass spectrometric analysis described below.

Tandem MS/MS Analysis of the Peptides Containing Asn-105—The daughter ion spectra were obtained in the triple-quadrupole daughter ion scan mode by introducing the peptides containing Asn-105 from Q1 into a collision cell (Q2) and observing the daughter ions in Q3. Q1 was locked on *m/z* 490.4 or 490.8. Q3 was scanned from 100 to 900 amu with a step size of 0.2 amu and with a dwell time of 1 ms/step. Ion-spray voltage was set at 5 kV, and the orifice potential was 40–50 V.

RESULTS

Reactivation of FAc-DEX D105N—FAc-DEX D105N showed a slight dehalogenation activity when determined immediately after ammonium sulfate precipitation (relative specific activity, usually 4.5% of that of the wild-type enzyme). The activity increased and reached 10.7% of the wild-type enzyme activity after storage at 4°C for 220 h; practically no increase was observed when stored at -30°C (Fig. 11). Incubation with fluoroacetate did not promote the autoactivation rate of FAc-DEX D105N (data not shown).

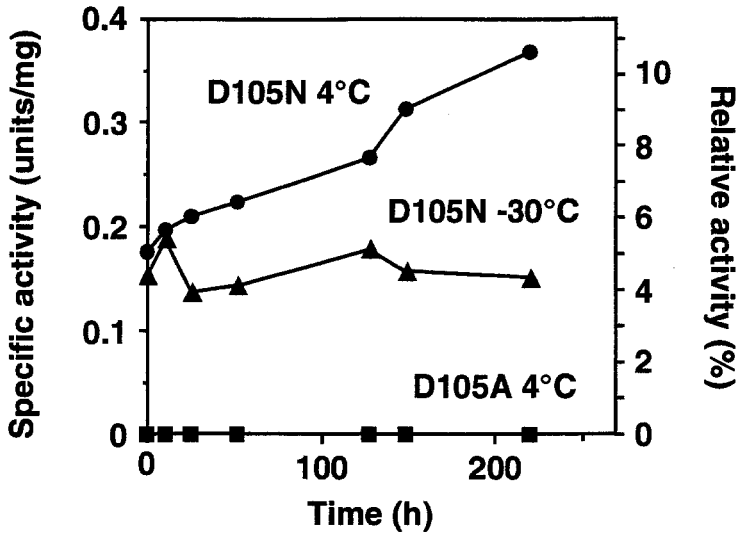

FIG. 11. **Reactivation of FAc-DEX D105N.** All samples were incubated in 50 mM potassium phosphate buffer (pH 7.5). ●, activity of FAc-DEX D105N enzyme incubated at 4°C; ▲, activity of the D105N enzyme incubated at -30°C; ■, activity of the D105A enzyme incubated at 4°C.

The wild-type enzyme undergoes paracatalytic inactivation: when the enzyme was incubated with hydroxylamine in the presence of fluoroacetate, the activity was significantly lost. The inactivation is caused by modification of the nucleophile Asp-105 by hydroxylamine (Chapter II). The activity of the D105N preparation was significantly lost when it was incubated with hydroxylamine in the presence of fluoroacetate, whereas it was fully retained when incubated with hydroxylamine in the absence of fluoroacetate (data not shown). The paracatalytic inactivation of the D105N preparation by hydroxylamine suggests that side-chain amide of Asn-105 is spontaneously converted to carboxylate.

Determination of Asp/Asn-105 Containing Peptides—To examine if Asn-105 is converted to Asp, wild-type FAc-DEX, the fresh preparation of the D105N enzyme, and the D105N enzyme incubated in 40 µl of 0.1 M Tris-sulfate buffer (pH 9.5) at 37°C for 96 h were digested with the modified trypsin, and the resultant peptide fragments were separated by HPLC and analyzed by ion-spray mass spectrometry. When the spectrometer was in the single-quadrupole mode, the total ion current chromatogram of the wild-type enzyme displayed several peaks. One of them which was eluted at 15.12 min (Fig. 12A, Peak 1) contained two ions at *m/z* 980.8 and 491.1, which are $[M + H]^+$ and $[M + 2H]^{2+}$ ions, respectively, and were assigned to the octapeptide Phe-99–Arg-106 (Fig. 13A). HPLC elution profile of the peptides derived from the fresh D105N preparation not incubated in Tris buffer gave a peak at 14.72 min (Peak 2) in addition to the peak at 15.12 min (Peak 3) (Fig. 12B). Peak 2 contained two ions of *m/z* 979.7 and 490.6, which are $[M + H]^+$ and $[M + 2H]^{2+}$ ions, respectively, and were assigned to the octapeptide Phe-99–Arg-106 containing

FIG. 12. **HPLC elution profiles of tryptic peptides.** Wild-type FAc-DEX (A), the fresh D105N preparation (B), and the D105N preparation incubated at pH 9.5 at 37°C for 96 h (C) were digested with the modified trypsin, and the resultant peptide fragments were separated by HPLC. Elution profiles from 14.0 min through 15.5 min are shown.

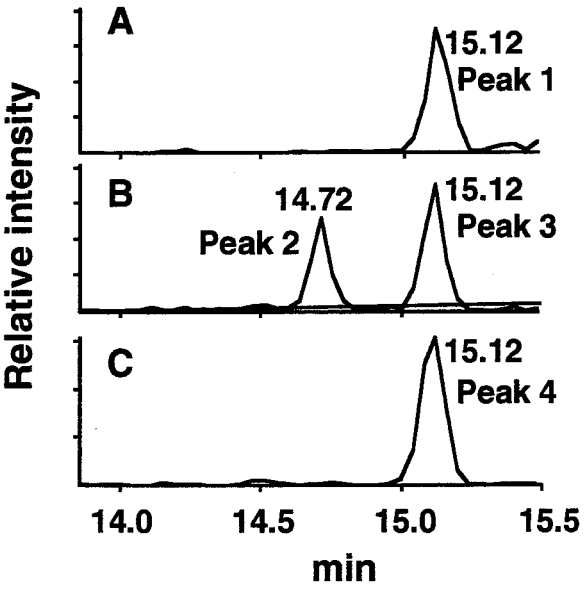

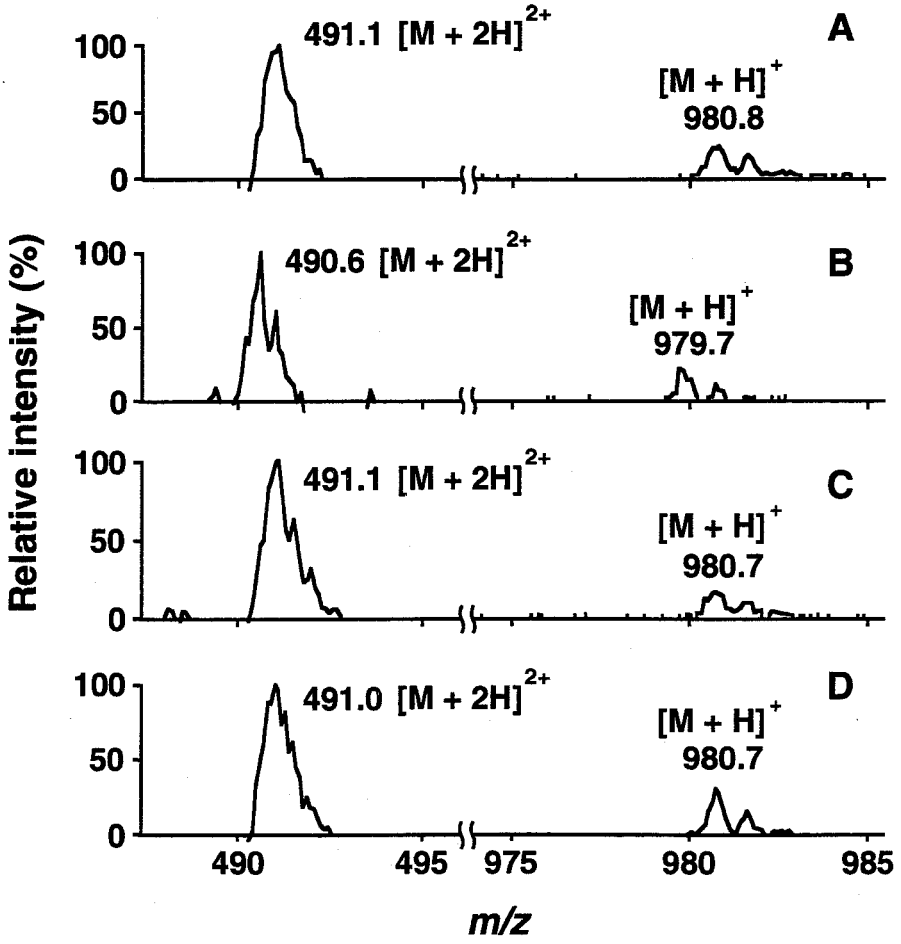

FIG. 13. **Ion-spray mass spectra of the peptides containing Asp/Asn-105.** Ion-spray mass spectra of Peak 1–4 in Fig. 12 are shown in A–D, respectively. Peak 1, 3, and 4 contained a monovalent ion at *m/z* 980.7–980.8 and a bivalent ion at *m/z* 491.0–491.1. Peak 2 contained a monovalent ion at *m/z* 979.7 and a bivalent ion at *m/z* 490.6, which are about 1.0 and 0.5 *m/z* units lower, respectively, than those of the corresponding ions derived from other Peaks.

Asn-105 (Fig. 13B). Peak 3 contained an $[M + H]^+$ ion at *m/z* 980.7 and an $[M + 2H]^{2+}$ ion at *m/z* 491.1, which were 1.0 and 0.5 *m/z* units higher, respectively, than those of the corresponding ions derived from Peak 2 (Fig. 13C). Since these ions derived from Peak 3 are virtually identical to those from Peak 1, Peak 3 is probably the octapeptide Phe-99–Arg-106 containing Asp-105. Thus, I have found that a side-chain amide of Asn-105 was converted to a side-chain carboxylate of Asp-105. The relative amount of the octapeptide containing Asp-105 derived from the D105N preparation is expected to increase when the mutant enzyme is incubated at high pH conditions. HPLC elution profile of the peptides derived from the D105N preparation incubated in Tris buffer (pH 9.5) at 37°C for 96 h gave a peak at 15.12 min (Peak 4), which is identical to the elution time of Peak 1 and Peak 3, whereas no peak was found around 14.72 min. Peak 4 provided an $[M + H]^+$ ion at *m/z* 980.7 and an $[M + 2H]^{2+}$ ion at *m/z* 491.0 (Fig. 13D), which are virtually identical to the mass spectra of Peak 1 and Peak 3 (Fig. 13A, C). These results indicate that Asn-105 is deamidated in a time-dependent manner to produce Asp.

To determine the amino acid residue in the D105N enzyme where mass increment occurred, tandem MS/MS analyses of the peptides of Peak 2 and Peak 4 (Peptide 2 and Peptide 4, respectively) were carried out. The daughter ions produced from Peptide 2 and Peptide 4 are shown in Fig. 14A and B, respectively. The Y series monovalent ions at *m/z* 695.2, 582.4, 483.2, 426.2, and 289.2 derived from Peptide 2 were assigned as Leu–Val–Gly–His–Asn–Arg, Val–Gly–His–Asn–Arg, Gly–His–Asn –Arg, His–Asn–Arg, and Asn–Arg, respectively (Fig. 14A). The ions produced from Peptide 4 at *m/z* 696.2, 583.1, 484.0, 427.0, and 290.0 were about 1 Da higher than the corresponding ions derived from Peptide 2 (Fig. 14B). However, the molecular mass of the fragment ion for the C-terminal Arg derived from Peptide 2 (*m/z* 175.2) was virtually identical to that from Peptide 4 (*m/z* 175.1). These results indicate that the modification causing 1-Da increase in Peptide 4 occurs at the position next to the C-terminal Arg, Asn-105. Peptides 2, Peptide 3, and Peptide 4 were isolated and sequenced with the Shimadzu protein sequencer. Peptide 2 gave the following sequence (the boldface indicates the amino acid at residue number 105): Phe–His–Leu–Val–Gly–His–**Asn**–Arg, which is identical to that predicted from the nucleotide sequence. Sequencing analyses of both Peptide 3 and Peptide 4 gave the following sequence: Phe–His–Leu–Val–Gly–His–**Asp**–Arg. In conclusion, the side-chain amide of Asn-105 undergoes nucleophilic attack of a water molecule to be converted to carboxylate.

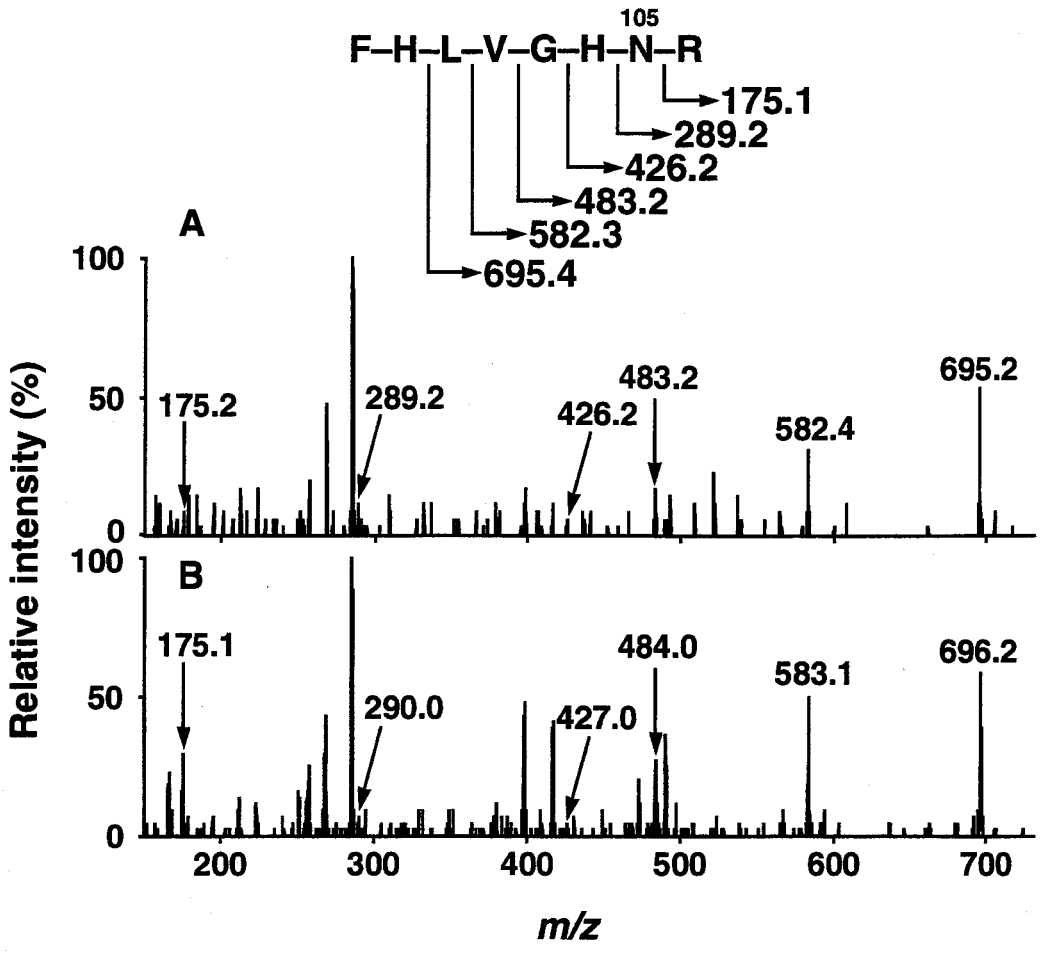

FIG. 14. **Tandem MS/MS daughter ion spectra of the octapeptides Phe-99–Arg-106 in Peak 2 and Peak 4 in Fig. 12 derived from the D105N preparation.** The calculated molecular mass of each fragment produced from the native octapeptide including Asn-105 is indicated in the sequence of the peptide. A, Peptide 2 (the parent ion: *m/z* 490.4 [divalent ion]). B, Peptide 4 (the parent ion: *m/z* 490.8 [divalent ion]).

DISCUSSION

Deamidation of Asn mutagenetically substituted for Asp acting as a nucleophile has been reported. Pries et al. showed that DhlA D124N yields the wild-type enzyme by prolonged storage under neutral to basic pH conditions (67). Similar autoactivation was observed for MEH D226N (68) and L-DEX YL D10N (Chapter IV). Recently, Xiang et al. have reported that D145N mutant of 4-CBA-CoA dehalogenase, in which Asp-145 acts as a nucleophile, is converted to the wild-type enzyme in such a way as deamidation of Asn-145 to Asp is accelerated by nucleophilic attack by a product, 4-hydroxy-benzoyl-CoA, generated by the wild-type enzyme produced by spontaneous deamidation: the deprotonated 4-hydroxy group of the product nucleophilically attacks the side-chain carbonyl carbon of Asn-145, followed by release of ammonia to form acetyl-oxy-benzoyl-CoA, which is subsequently hydrolyzed to the wild-type enzyme and 4-hydroxy-benzoyl-CoA (69). I have shown in this chapter that the activity of the FAc-DEX D105N preparation increased in a time- and temperature-

dependent manner owing to the deamidation of Asn-105 to generate the wild-type enzyme (Fig. 11, p.33). Incubation with fluoroacetate did not promote the deamidation (data not shown). Asn-105-containing tryptic peptide in which succinimidyl intermediate is formed was not found. These results indicate that Asn-105 of FAc-DEX D105N is spontaneously deamidated to produce Asp.

The following four factors are probably responsible for the deamidation of Asn-105. The first one is activation of a water molecule that attacks the side-chain amide. In the wild-type FAc-DEX reaction, a water molecule activated by His-272 attacks the carbonyl carbon of the ester bond causing release of glycolate and regeneration of the side-chain carboxylate of Asp-105 (Scheme 3, p.15). A water molecule is probably activated in the D105N enzyme in the same manner as in the wild-type enzyme, and is responsible for the amide hydrolysis. The second factor is the position of the activated water. The least energy-demanding direction of approach of the activated water molecule to the amide carbon atom is from above (or below) the substantially planar structure of the amide. The water molecule involved in the deamidation is probably positioned where it can easily attack the planar structure of the amide. The third factor that affects the deamidation rate is the presence of an oxyanion hole that stabilizes the negative charge that develops on the oxygen atom of the side-chain amide of Asn-105 during the hydrolysis. According to the three-dimensional structure of FAc-DEX built by homology modeling using the structures of DhlA and BpoA2 (Fig. 10B, p.29), the hydrogens bound to the main-chain nitrogens of Arg-106 and Phe-35 can be positioned to form hydrogen-bonds to stabilize the negative charge. The fourth factor would be the presence of proton-donating residue(s) in the vicinity of the amino group of the side-chain amide, facilitating the elimination of the amino group as ammonia. According to the homology modeling of FAc-DEX, Arg-106, Arg-109, and His-104 can be present around Asn-105 and possibly donate proton to the amido-nitrogen of Asn-105 (Fig. 10B).

The deamidation efficiency upon incubation at pH 7.5 at 4°C is markedly different between the mutant enzymes, DhlA D124N, FAc-DEX D105N, and L-DEX YL D10N, although the deamidation mechanisms of these mutant enzymes are considered to be similar to each other: DhlA D124N activity increased from 27% to nearly 100% over a period of 400 h (67); FAc-DEX D105N activity increased from 4.5% to 10.7% over a period of 220 h (Fig. 11, p.33); L-DEX YL D10N activity increased from 1% to 3.6% over a period of 3 months (Chapter IV). These enzymes are probably different from each other in the nucleophilicity and position of a water molecule that attacks the asparagine residue, in the properties of the oxyanion hole, and in the architecture of amino acid residues providing a proton to the amido-nitrogen of the asparagine residue.

SUMMARY

FAc-DEX catalyzes the hydrolytic dehalogenation of fluoroacetate and other haloacetates. I have shown that Asp-105 of the enzyme acts as a nucleophile to attack the α-carbon of haloacetate to form an ester intermediate, which is hydrolyzed by a water molecule activated by His-272 to produce glycolate (Chapter I). Thus replacement of Asp-105 by other amino acid residue such as Ala, Gly, and Val results in total inactivation. In contrast, replacement by Asn does not completely inactivate the enzyme. Moreover, the activity of the D105N preparation increased in a time-dependent manner. Ion-spray mass spectrometric analyses and amino acid sequence analysis showed that deamidation of Asn-105 occurred to produce the wild-type enzyme, which is responsible for the activity of the mutant preparation. These results indicate that the deamidation of Asn probably occurs by direct attack of a water molecule that acts as a nucleophile in hydrolysis of an ester intermediate in the wild-type enzyme reaction.

CHAPTER IV

The Cyanoalanine Residue as an Intermediate Structure in the Catalytic Reaction of L-2-Halo acid Dehalogenase D10N Mutant: Identification by Mass Spectrometric Monitoring of the Enzyme Reaction

INTRODUCTION

L-DEX YL catalyzes the hydrolytic dehalogenation of L-2-haloalkanoic acids to produce the corresponding D-2-hydroxyalkanoic acids with inversion of the C2-configuration (12). The reaction proceeds via a nucleophilic attack of a carboxylate oxygen of Asp-10 on the α-carbon atom of various L-2-haloalkanoic acids, causing the release of a halide ion and the formation of an ester intermediate (Scheme 7, V), which is subsequently hydrolyzed (16, 17). In the X-ray structure, there is a water molecule close to Asp-10, Ser-175, Asn-177, and Asp-180, the latter three of which are supposed to enhance the nucleophilicity of the water molecule for hydrolysis of the ester intermediate (Scheme 7; 20, 21). Replacement of the catalytic nucleophile, Asp-10, by Ala, Gly, Ser, and Glu yielded mutant enzymes showing no dehalogenation activity. However, replacement of Asp-10 by Asn did not completely inactivate the enzyme (15).

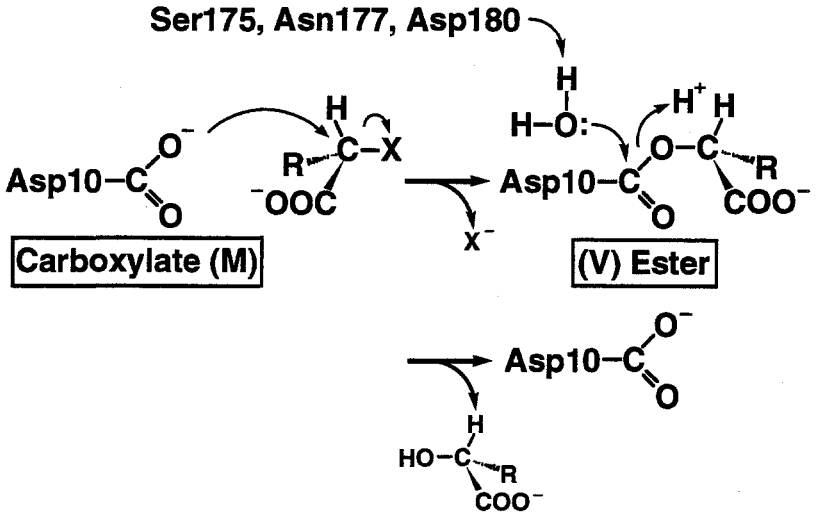

Scheme 7. **Reaction mechanism of L-DEX YL.**

The reactions catalyzed by DhlA (22) and MEH (41) also proceed via an ester intermediate, although little sequence similarity is found between these enzymes and L-DEX YL. In the reactions catalyzed by DhlA and MEH, Asp-124 and Asp-226 act as a nucleophile, respectively. Pries et al. have reported that DhlA D124N undergoes time- and pH-dependent autoactivation, in which Asn-124 is spontaneously converted into Asp (67). Laughlin et al. have shown autoactivation of MEH D226N mutant (68).

The deamidation of Asn probably occurs by direct attack of a water molecule that acts as a nucleophile in hydrolysis of an ester intermediate in the wild-type enzyme reaction.

In the present study, I have analyzed the mechanism of dehalogenation catalyzed by the L-DEX YL D10N preparation. I have found that Asn-10 of the D10N mutant enzyme is spontaneously deamidated to produce Asp, though slowly. Thus the preparation contains the wild-type enzyme besides the D10N enzyme itself, and both of these enzymes could contribute to the dehalogenation activity. This makes it difficult to analyze the reaction catalyzed by the D10N enzyme itself by monitoring the chemical conversion of the substrate. Accordingly, I have decided to employ ion-spray mass spectrometry to monitor the structural change of the D10N enzyme upon incubation with the substrate. The D10N enzyme constitutes a major part of the enzyme preparation, and the small amount of the wild-type enzyme contaminating the preparation does not interfere with the mass spectra of the D10N enzyme. As a result, I have found that the D10N mutant enzyme itself catalyzes dehalogenation, and that Asn-10 undergoes a unique structural change in the course of the catalysis: Asn-10 is converted into β-cyano-L-alanine (β-CNAla) residue via an imidate, and then regenerated in the catalytic cycle. This is the first example of formation of β-CNAla residue as an enzyme reaction intermediate.

EXPERIMENTAL PROCEDURES

Materials—Lysyl endopeptidase of *Acromobacter lyticus* M497-1 and phenylisothiocyanate were purchased from Wako Pure Chemical Industries (Osaka, Japan), L-2-chloropropionic acid (L-CPA), L-asparagine, L-aspartic acid, and DL-alanine from Nacalai Tesque (Kyoto, Japan), β-CNAla from Sigma (St. Louis, MO), and $H_2{}^{18}O$ (94–97%) from Isotec (Dayton, OH). All other chemicals were of analytical grade.

Enzyme Preparation—Replacement of amino acid residue(s) was carried out by the method of Kunkel (46). Mutant genes for D10N and D180N were constructed as reported previously (15). The synthetic mutagenic primer designed for the D10N/L11K double mutant was as follows (the underlines indicate the mutagenized nucleotides):

5'-CAGCGTACCGTACTTGTTGAAGGCAATACC.

The substitutions were confirmed with the protein sequencer, DNA sequencer, and the ion-spray mass spectrometer, PE-Sciex API 300. Mutant enzymes were produced in *E. coli* JM109. The recombinant *E. coli* cells producing the enzyme were grown aerobically at 37°C for 14 h in LB medium containing 200 μg/ml ampicillin and 0.2 mM isopropyl-1-thio-β-D-galactoside. The cells harvested from a 4-l culture were disrupted by sonication. The supernatant was fractionated with ammonium sulfate. A fraction of 40–70% saturation was dissolved in the standard buffer, and then applied to

the Butyl-Toyopearl 650 column (3 × 25 cm). The column was washed with 500 ml of the buffer supplemented with 30% (w/v) ammonium sulfate, and the enzyme was eluted with a linear gradient of 30–20% ammonium sulfate in the buffer with a total volume of 1 liter. The fractions containing the mutant enzyme were identified by SDS-PAGE, dialyzed against 10 mM potassium phosphate (pH 7.5), and applied to the DEAE-Toyopearl 650M column (1.7 × 5 cm) equilibrated with the same buffer. The enzyme was eluted with a linear gradient of 10–50 mM potassium phosphate (pH 7.5) with a total volume of 200 ml. The fractions containing the mutant enzyme were pooled and used as a purified preparation of the mutant enzyme.

Determination of the Enzyme Activity—L-DEX YL was routinely assayed by determination of chloride ions produced from L-CPA by the method of Iwasaki et al. (47). The standard assay mixture (100 µl) contained 2.5 µmol of L-CPA, 10 µmol of Tris-sulfate buffer (pH 9.5), and the enzyme. The reaction was terminated by addition of 10 µl of 1.5 M sulfuric acid after incubation at 30°C for 10 min. One unit of the enzyme was defined as the amount of the enzyme that catalyzes dehalogenation of 1 µmol of L-CPA per min.

Identification of Products of Edman Degradation of β-CNAla—Manual Edman degradation of authentic amino acids was carried out (70, 71). Authentic Ala (1.2 mg), Asn (2.6 mg), Asp (1.6 mg), and β-CNAla (1.7 mg) were separately dissolved in 60% pyridine containing 1.5% dimethylallylamine, mixed with 20 µl of phenylisothiocyanate, and incubated anaerobically at 45°C for 40 min. Remaining phenylisothiocyanate was removed with benzene, and the resultant phenylthiocarbamyl derivatives were lyophilized. The lyophilized samples were mixed with 20 µl of trifluoroacetic acid and incubated anaerobically at 15°C for 15 min. The resultant 2-anilino-5-thiazolinone derivatives were extracted with ethyl acetate, dried, and converted to the phenylthiohydantoin(PTH)-amino acids by incubating with 1 N hydrochloric acid at 80°C for 8 min. The PTH-amino acids were extracted with ethyl acetate, dried, and used for identification and quantification. The dried PTH-amino acids were dissolved in 40% acetonitrile containing 10 mM acetic acid, and loaded onto an ODS reverse phase column for separation of PTH-amino acids (Wakopak WS-PTH column, 4.6 × 250 mm) connected to the mass spectrometer, PE-Sciex API 365. Elution was carried out with 40% acetonitrile containing 0.1% formic acid at a flow rate of 45 µl/min. The total ion current chromatogram was recorded in the single-quadrupole mode. The quadrupole was scanned from 200 to 1,000 amu with a step size of 0.1 amu and with a dwell time of 0.5 ms/step. The ion-spray voltage was set at 5 kV, and the orifice potential was 50 V. The molecular mass of each peptide was calculated using the Bio-MultiView software. The HPLC fractions were collected and further analyzed by the same chromatography protocol used in the Shimadzu protein sequencer.

Determination of Molecular Masses of Wild-type L-DEX YL, D10N, D10N/L11K, and D10N/D180N Incubated with L-CPA—Wild-type L-DEX YL, the D10N mutant enzyme, the D10N/L11K double mutant enzyme, or the D10N/D180N double mutant enzyme (10 nmol each) was incubated with L-CPA in the standard assay mixture. The reaction was terminated with 10 μl of 20% (v/v) formic acid, followed by centrifugation at 8200 *g* for 1 min. The enzyme was deionized with Jasco HPLC system (Tokyo) with the C_{18} reverse phase column (Shiseido Capcell Pak, SG 300 Å 5 μm, 4.6 × 250 mm) at room temperature, employing linear gradients of solvent A (0.1% formic acid) and solvent B (acetonitrile containing 0.1% formic acid): sample injection; 3 min, 20% B; 12 min, 20–100% B; 3 min, 100% B; 2 min, 100–20% B (flow rate: 1 ml/min). The deionized enzyme was lyophilized, dissolved in 50% acetonitrile containing 0.05% formic acid, and introduced into the mass spectrometer, PE-Sciex API 300 or API 365 at a flow rate of 2.5 μl/min. The quadrupole was scanned from 300–800 to 2,000 amu with a step size of 0.1–0.2 amu and with a dwell time of 0.208–1 ms/step. The orifice potential was set at 30–60 V.

Digestion of the D10N/L11K Mutant Enzyme with Lysyl Endopeptidase—The enzyme incubated and deionized as described above was lyophilized, dissolved in 50 μl of 8 M urea in 200 mM Tris-sulfate buffer (pH 7.2), and incubated at 37°C for 1 h. The enzyme was then digested by addition of 82.5 pmol of lysyl endopeptidase dissolved in 75 μl of 1 M Tris-sulfate buffer (pH 9.0) at 37°C for 12 h.

Reaction of the D10N/L11K Mutant Enzyme with L-CPA in $H_2{}^{18}O$—The D10N/L11K mutant enzyme (10 nmol) in 17 μl of 50 mM potassium phosphate buffer (pH 7.5) was lyophilized. The lyophilized enzyme was dissolved in 40 μl of $H_2{}^{18}O$ containing 2.5 μmol of L-CPA and 10 μmol of Tris-sulfate (pH 9.5), and incubated at 30°C for 60 min. The reaction was terminated by lyophilization. The lyophilized enzyme was denatured with 20 μl of 8 M urea dissolved in 200 mM Tris-sulfate buffer (pH 7.2) prepared with $H_2{}^{18}O$, and digested with lysyl endopeptidase dissolved in 20 μl of 1 M Tris-sulfate buffer (pH 9.0) prepared with $H_2{}^{18}O$ at 37°C for 15 h.

LC/MS Analysis of the Peptides Containing Asn-10—The proteolysates (95–100 μl) were loaded onto the C_{18} column connected to the mass spectrometer, PE-Sciex API 300 or 3000. Elution was carried out with 2% acetonitrile containing 0.1% formic acid for 5 min, followed by a linear gradient of 2–82% acetonitrile containing 0.1% formic acid over 40 min at a flow rate of 40 μl/min. The quadrupole was scanned from 150–200 amu to 1,000 amu with a step size of 0.2 amu and with a dwell time of 0.5 ms/step. The orifice potential was set at 50 V. For detailed analysis of the peptides containing Asn-10, the HPLC fractions were collected, concentrated, and injected into the mass spectrometer for tandem MS/MS analysis described below.

Tandem MS/MS Analysis of the Peptides Containing Asn-10—The daughter ion spectra were obtained in the triple-quadrupole daughter ion scan mode by introducing

the peptides containing Asn-10 from Q1 into a collision cell (Q2) and observing the daughter ions in Q3. Q1 was locked on *m/z* 631.4, 649.5, 653.3, 655.3, 722.6, or 724.5. Q3 was scanned from 10–120 to 700–1,000 amu with a step size of 0.1 amu and with a dwell time of 0.5–1.0 ms/step. The orifice potential was set at 40–68 V.

RESULTS

Mass Spectrometric Analysis of Wild-type L-DEX YL Incubated with L-CPA—I have found that structural changes of L-DEX YL in the course of the catalytic reaction can be monitored by ion-spray mass spectrometry. The mass spectral change of the enzyme upon incubation with L-CPA is shown in Fig. 15. The control enzyme not incubated with L-CPA showed a peak at 26,182 Da (M), which is virtually identical to the value predicted from the nucleotide sequence (26,179 Da): an error of ± 3 Da is acceptable in analysis of a protein around 26 kDa with the mass spectrometer used. After 4 sec of the incubation, the original peak almost disappeared, and a new peak appeared at 26,255 Da (M+73), which is considered to be an ester intermediate (M+72) (Scheme 7, V, R = CH_3, p.39). The difference between the measured increment (+73) and the estimated one (+72) can be attributed to a measurement error. The original peak (M) increased over a period from 4 to 20 sec and became predominant eventually, while the M+73 peak decreased and disappeared. This result indicates that most of the substrates had been degraded before this time by the enzyme reaction, and the rate of formation of the ester intermediate became slower than the rate of degradation of the intermediate.

The reaction mixture for the present experiment initially contained 2.5 μmol of L-CPA at 25 mM. Since the k_{cat} value of the enzyme for hydrolysis of L-CPA is 47 sec^{-1} (15), 2.5 μmol of L-CPA is degraded in about 5.3 sec with 10 nmol of the enzyme when the substrate is present at a concentration much higher than the K_m value of the enzyme (0.37 mM). Thus it is reasonable that the concentration of the substrate became low enough to cause the decrease in the rate of formation of the ester intermediate in about 4 sec as observed in Fig. 15.

Reactivation of the D10N Enzyme—I have found that every D10N preparation shows a slight dehalogenation activity when determined immediately after purification (relative specific activity, usually 1% of that of the wild-type enzyme). The activity increased in a time- and temperature-dependent manner. It showed 3.6% and 6.2% of the wild-type enzyme activity after storage at 4°C for 2 and 3 months, respectively; when stored at room temperature for about a month, it showed 26% of the wild-type enzyme activity. Automated Edman degradation of the D10N preparation showing 26% of the wild-type enzyme activity revealed the occurrence of large quantity of Asp at the position of Asn-10 (data not shown). These results indicate that side-chain amide of Asn-10 is spontaneously deamidated to produce carboxylate.

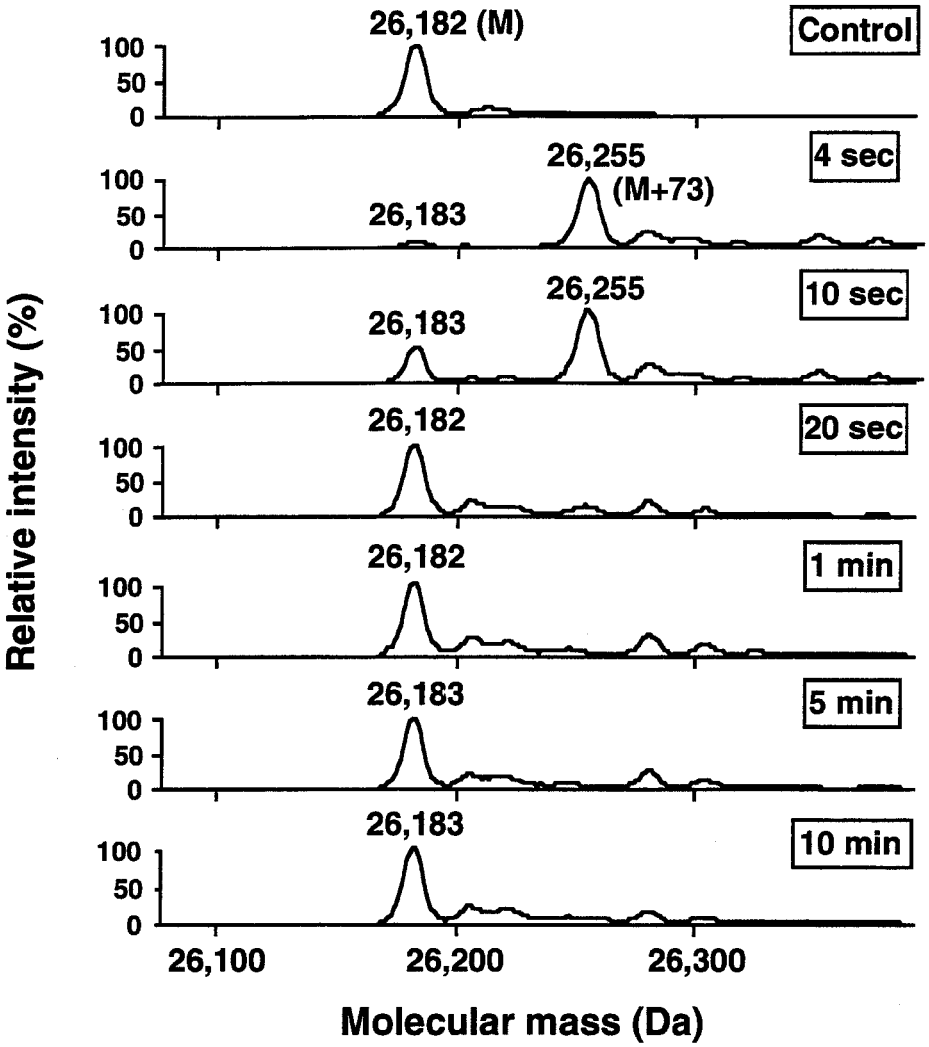

FIG. 15. **Structural change of wild-type L-DEX YL incubated with L-CPA.** Wild-type L-DEX YL was incubated with L-CPA for indicated times, denatured by addition of formic acid, deionized by HPLC, and analyzed by ion-spray mass spectrometry.

Mass Spectrometric Analysis of D10N Incubated with L-CPA—Although the D10N preparation contains the wild-type enzyme as described above, its amount in the fresh preparation is considered to be at most 1% of the total enzyme judging from the specific activity of the preparation. Thus it is possible to monitor the structural change of the D10N enzyme itself by mass spectrometry, because the small amount of the wild-type enzyme does not interfere with the mass spectra of the D10N enzyme, which is present abundantly. I have determined molecular masses of the D10N enzyme incubated with L-CPA for indicated times shown in Fig. 16 in the same manner as the wild-type enzyme. The control enzyme not incubated with L-CPA showed a peak at 26,180 Da (M), which is virtually identical to the value predicted from the nucleotide sequence (26,178 Da). After 10 sec of the incubation, the original peak disappeared, and new peaks appeared at 26,253 Da (M+73) and 26,162 Da (M-18). As the relative abundance of the M+73 species decreased, the M-18 species increased over a period from 10 sec to 1 min. The enzyme occurred predominantly as

the M-18 variant from 20 sec to 40 min. The original peak (M) reappeared and increased over a period from 30 to 60 min, and became predominant by 60 min. When monochloroacetate instead of L-CPA was used as a substrate, a species showing 60-Da increase instead of M+73 species was observed (data not shown), indicating that a covalently linked enzyme–substrate intermediate is produced in the course of the reaction.

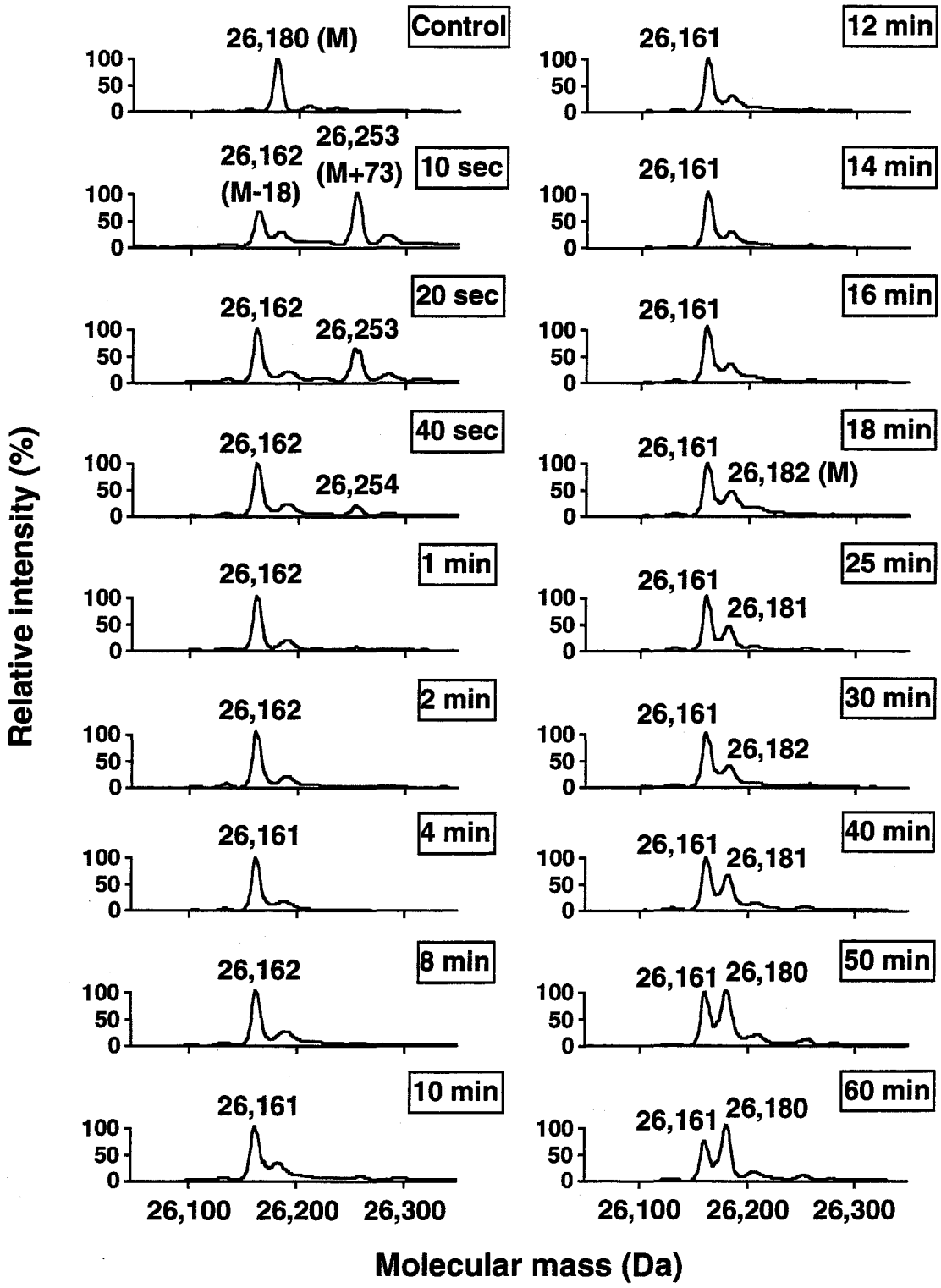

FIG. 16. **Structural change of the D10N mutant enzyme incubated with L-CPA.** The enzyme was incubated with L-CPA for indicated times and analyzed in the same manner as described in the legend of Fig. 15.

Two probable mechanisms can be delineated for the structural change of the D10N enzyme (Scheme 8 and 9). The first one is shown in Scheme 8: Asn-10 attacks L-CPA to form an asparagine β-imidate 1-carboxyethyl ester (VI, M+72), and a proton and D-lactic acid are eliminated from the imidate to produce a nitrile (VII, M-18), which is subsequently hydrolyzed to reproduce Asn-10 (M). The difference between the measured (+73) and the estimated (+72) mass increments can be attributed to measurement error or to the conversion of the imidate to an aspartate 1-carboxyethyl ester as shown in Scheme 10 (IX, M+73) upon denaturation of the enzyme with formic acid. In the second probable mechanism shown in Scheme 9, the imidate intermediate is produced in the same manner as shown in Scheme 8, followed by formation of an intramolecular cross-link (VIII, M-18) caused by nucleophilic attack by hydroxyl group of Ser or Thr positioned in the vicinity of the imidate.

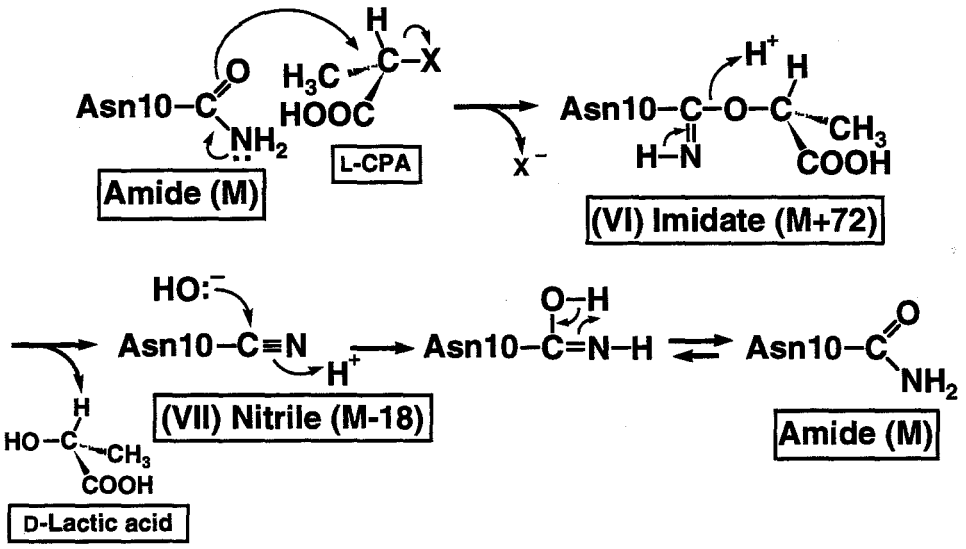

Scheme 8. **Possible mechanism for the structural change of L-DEX YL D10N involving an imidate and a nitrile as enzyme-reaction intermediates.**

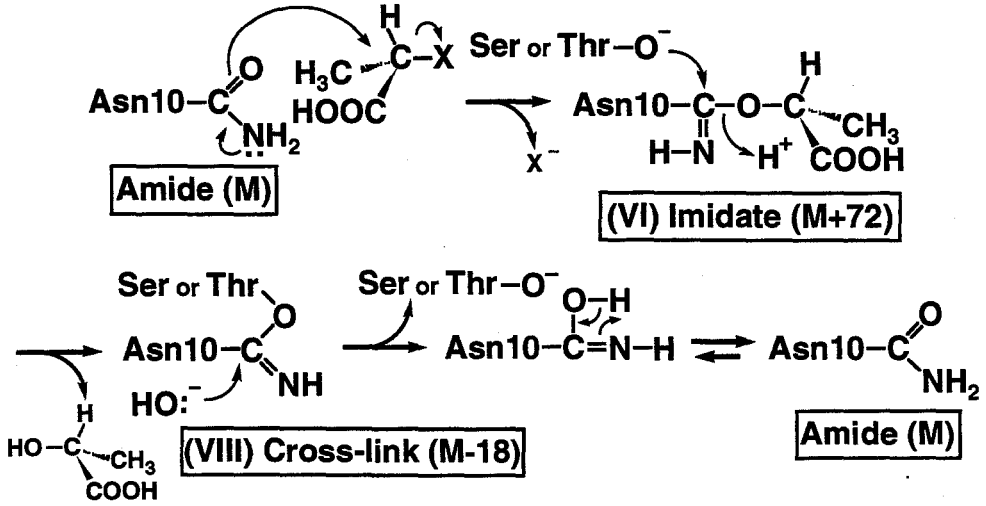

Scheme 9. **Possible mechanism for the structural change of L-DEX YL D10N involving an imidate and a cross-link as enzyme-reaction intermediates.**

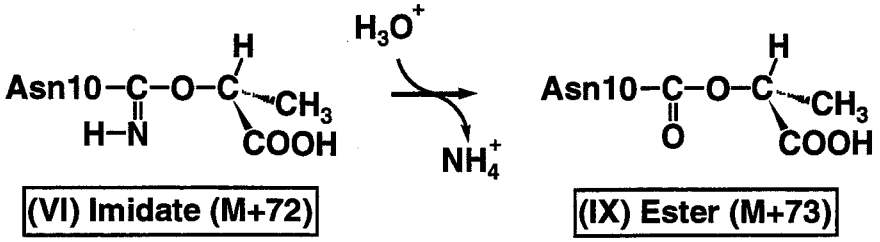

Scheme 10. **Conversion of the imidate into the ester by acid-catalyzed hydrolysis.**

Construction, Purification, and Characterization of the D10N/L11K Mutant Enzyme—D10N/L11K was constructed by site-directed mutagenesis to produce a lysyl-endopeptidase hydrolytic site adjacent to Asn-10. It was purified to homogeneity, and the substitutions were confirmed by amino acid sequencing, DNA sequencing, and ion-spray mass spectrometry. The mass spectrum showed a peak at 26,195 Da (M'), which is virtually identical to the value predicted from the nucleotide sequence, 26,193 Da. It was confirmed that the M'+73 (26,268 Da) and the M'-18 (26,177 Da) variants were formed when the D10N/L11K enzyme was incubated with L-CPA for 10 sec and 8 min, respectively (data not shown). Thus the Lys residue introduced next to the C-terminal side of Asn-10 has little effect on the reactivity of the enzyme.

Determination of the Structure Causing 73-Da Increase—To examine if Asn-10 was modified during the incubation with L-CPA, I have carried out amino acid sequencing. The native D10N enzyme gave the following sequence (the boldface indicates the 10th amino acid residue): Met–Asp–Tyr–Ile–Lys–Gly–Ile–Ala–Phe–**Asn**–Leu, which is identical to that predicted from the nucleotide sequence. Sequencing analysis of the M+73 variant gave the following result: Met–Asp–Tyr–Ile–Lys–Gly–Ile–Ala–Phe–**X**–Leu, in which X is an amino acid residue whose retention time is different from that of every common animo acid residue including Asn, indicating that Asn-10 is modified in the M+73 variant.

The D10N/L11K enzyme was used to examine the modification of Asn-10 by ion-spray mass spectrometry. D10N/L11K incubated with (or without) L-CPA was digested with lysyl endopeptidase, and the resultant peptides were separated by HPLC and analyzed by ion-spray mass spectrometry. When the spectrometer was in the single-quadrupole mode, the total ion current chromatogram displayed several peaks: one of them was assigned as a derivative of hexapeptide Gly-6–Lys-11 (data not shown). Ion-spray mass spectrum of the hexapeptide derived from the native D10N/L11K had a peak at *m/z* 649.5, which was assigned as a positive monovalent ion (Fig. 17A, M'). The hexapeptide isolated from the enzyme incubated with L-CPA for 10 sec and denatured with formic acid showed a new peak at *m/z* 722.6, which is about 73 Da higher than that derived from the unmodified one (Fig. 17B, M'+73).

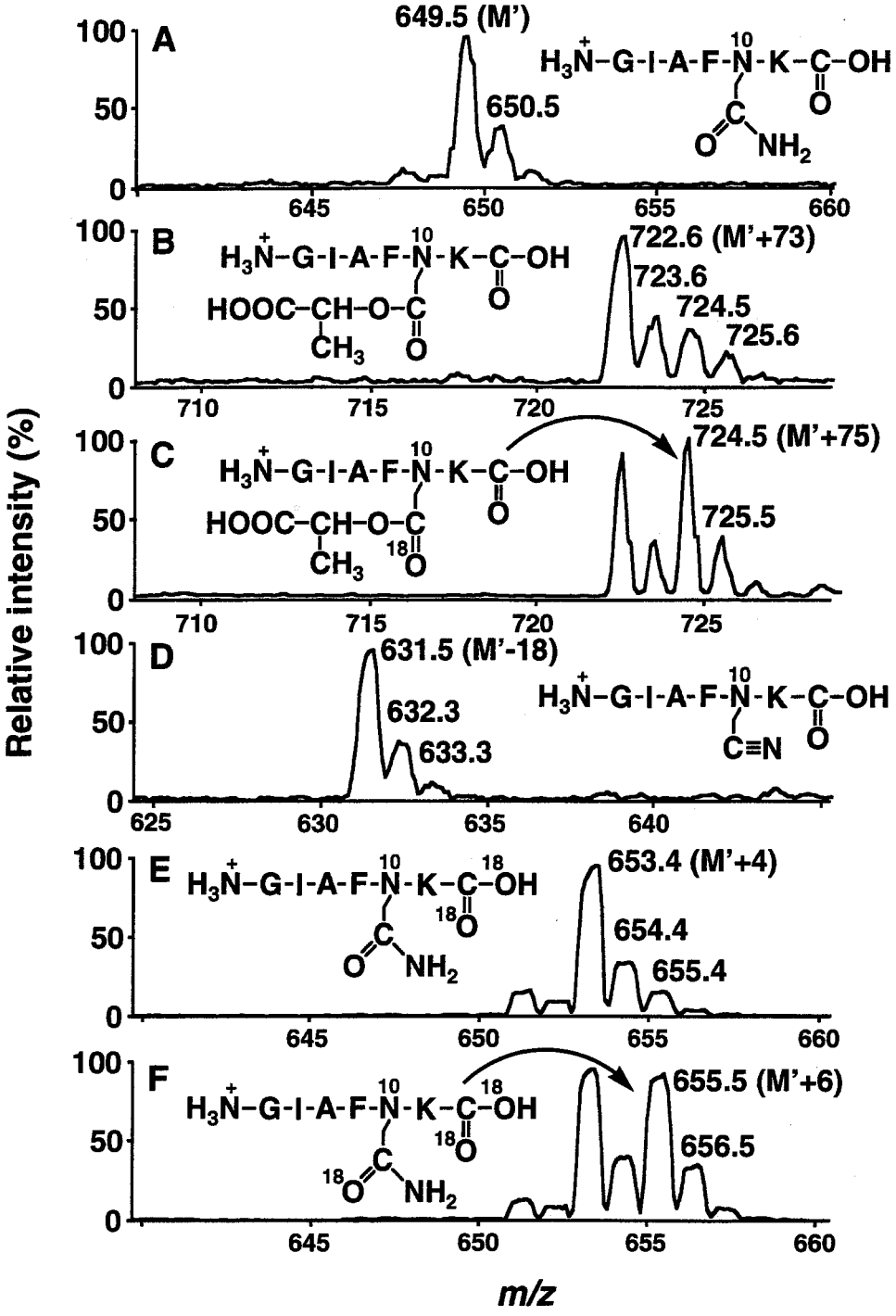

FIG. 17. **Ion-spray mass spectra of the peptides containing Asn-10.** Ion-spray mass spectra of the hexapeptides (Gly-6–Lys-11) derived from the D10N/L11K enzyme incubated with (B–D, F) or without (A, E) L-CPA. Incubation time is as follows: 0 min (A), 10 sec (B, C), 8 min (D), and 1 h (E, F). The denaturation of the enzyme with formic acid was carried out in $H_2{}^{16}O$ (A, B, D) or in $H_2{}^{18}O$ (C, E, F). Digestion with lysyl endopeptidase of the enzyme was carried out in $H_2{}^{16}O$ (A–D) or in $H_2{}^{18}O$ (E, F). Possible structures of the modified peptides are also shown.

To determine the amino acid residue where mass increment occurred, tandem MS/MS analysis of the M'+73 peptide was carried out. The daughter ions produced from the unmodified and the M'+73 peptides are shown in Fig. 18A and B, respectively. The

Y series monovalent ions at *m/z* 649.3, 479.0, 408.1, and 261.2 derived from the unmodified peptide were assigned as Gly–Ile–Ala–Phe–Asn–Lys, Ala–Phe–Asn–Lys, Phe–Asn–Lys, and Asn–Lys, respectively (Fig. 18A). The ions produced from the M'+73 peptide at *m/z* 722.6, 552.5, 481.2, and 334.4 were about 73 Da higher than the corresponding ions derived from the unmodified one, respectively (Fig. 18B). However, the molecular mass of the fragment ion for the C-terminal Lys derived from the M'+73 peptide (*m/z* 147.1) was virtually identical to that from the unmodified one (*m/z* 147.0). This result indicates that the modification causing 73-Da increase occurs at the position next to the C-terminal Lys, Asn-10.

Because 1-Da difference is significant around the mass range shown in Fig. 17 and Fig. 18, the exact mass increase in the M'+73 peptide at Asn-10 is 73 Da, not 72 Da. This indicates the presence of the ester, not the imidate, in the peptide. However, this result does not exclude a possibility that an imidate intermediate was actually produced in the reaction, because an imidate is readily hydrolyzed to an ester under low pH conditions (72; Scheme 10, p.47), which was employed in the present experiment to terminate the enzyme reaction. An ^{18}O atom is expected to be incorporated in the ester intermediate by addition of $H_2{}^{18}O$, if the presumed imidate intermediate is indeed hydrolyzed spontaneously by acidification. To examine if the observed ester is produced from the imidate, $H_2{}^{18}O$ was added to the reaction mixture at the termination of incubation. The mass spectrum showed a new peak at *m/z* 724.5 (Fig. 17C, M'+75), indicating that an oxygen atom of a solvent water molecule was introduced into the hexapeptide Gly-6–Lys-11. To determine the amino acid residue where the 2-Da increment occurred, tandem MS/MS analysis of the M'+75 peptide was carried out as described above. The Y series ions produced by fragmentations at the amino terminal side of Asn-10 in the M'+75 peptide were about 2 Da higher than the corresponding ions produced from the M'+73 peptide, while the molecular masses of C-terminal Lys derived from the two peptides were virtually identical (Fig. 18B and C). This indicates that the 2-Da mass increase occurred at Asn-10. No M'+75 peptide was produced when $H_2{}^{18}O$ was added to the reaction mixture at 1 min after the termination (data not shown), indicating that there is no exchange of an ^{18}O atom of $H_2{}^{18}O$ with a carbonyl oxygen of the ester bond. These results show that the oxygen atom of a water molecule was incorporated into the peptide at the position corresponding to Asn-10 upon denaturation with formic acid, supporting the view that an actual reaction intermediate is not the ester but the imidate as shown in Scheme 8 and Scheme 9 (p.46). The imidate was probably converted into the ester due to acid-catalyzed hydrolysis (Scheme 10, p.47).

Determination of the Structure Causing 18-Da Mass Decrease—I have analyzed the Edman-degradation products of authentic β-CNAla as described in "Experimental Procedures" by ion-spray mass spectrometry, and found that the reaction gave PTH-Asn as the most predominant product accompanying minor prod-

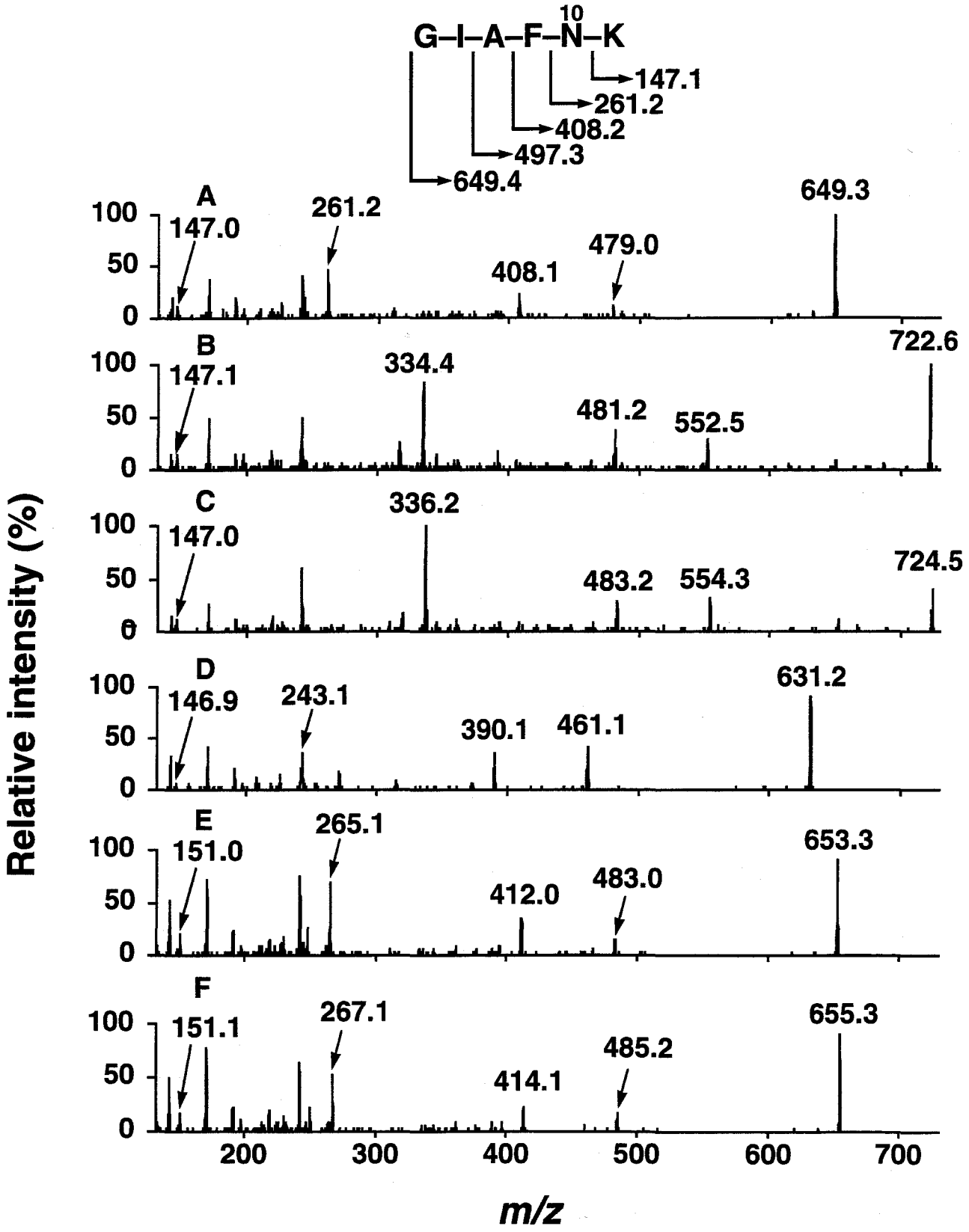

FIG. 18. **Tandem MS/MS daughter ion spectra of the unmodified and modified hexapeptides Gly-6–Lys-11.** The calculated molecular mass of each fragment derived from the native hexapeptide is indicated in the sequence of the peptide. A, the unmodified peptide (the parent ion: *m/z* 649.5). B, the M'+73 peptide (the parent ion: *m/z* 722.6). C, the M'+75 peptide (the parent ion: *m/z* 724.5). D, the M'-18 peptide (the parent ion: *m/z* 631.4). E, the M'+4 peptide (the parent ion: *m/z* 653.3). F, the M'+6 peptide (the parent ion: *m/z* 655.3).

ucts of PTH-Asp and PTH-β-CNAla (data not shown). A nitrile structure undergoes acid-catalyzed nucleophilic addition of water to produce an amide (73). Edman reaction employs strong acids such as trifluoroacetic acid and hydrochloric acid in the reaction cycle. Therefore the nitrile structure of β-CNAla is converted to an amide in the course of the reaction. Thus, even if a β-CNAla residue is formed in a peptide, it is converted to PTH-Asn during Edman degradation.

I have carried out amino acid sequencing of the M-18 variant of D10N. It gave the following sequence (the boldface indicates the 10th amino acid residue): Met–Asp–Tyr–Ile–Lys–Gly–Ile–Ala–Phe–**Asn**–Leu. Although this result may indicate that Asn-10 is intact in the M-18 variant, it is also consistent with the mechanism of β-CNAla formation at residue number 10 followed by spontaneous hydrolysis during Edman degradation.

To confirm the β-CNAla formation, the M'-18 variant of the D10N/L11K enzyme was digested, and the resultant peptides were separated and analyzed by ion-spray mass spectrometry. I have obtained a peptide with the *m/z* value of 631.5 (Fig. 17D, M'-18). This peak was identified as the hexapeptide Gly-6–Lys-11 in which the mass decreased by 18 Da. I have determined by tandem MS/MS analysis the amino acid residue which caused the mass reduction. The Y series ions produced by fragmentations at the amino terminal side of Asn-10 in the M'-18 peptide were about 18 Da lower than the corresponding ions produced from the unmodified one, while the molecular masses of C-terminal Lys derived from the two peptides were virtually identical (Fig. 18A and D). This result indicates that Asn-10 was specifically modified in such a way as its molecular mass becomes 18 Da lower than the original value. The most reasonable compound formed at residue number 10 in the M-18 (or M'-18) variant is a β-CNAla residue. Since nitrile can hardly be produced from the cross-link structure in the process of the mass spectrometry, the mechanism shown in Scheme 9 (p.46) is excluded.

Reconversion of β-CNAla to Asn-10—To examine if the final step of the reaction is reconversion of β-CNAla into Asn as shown in Scheme 8 (p.46), the D10N/L11K enzyme was incubated in $H_2{}^{18}O$ in the presence or absence of L-CPA for 60 min. If β-CNAla is reconverted to Asn as shown in Scheme 8, an ^{18}O atom is expected to be incorporated in the side-chain amide of Asn-10 only when the mutant enzyme is incubated with the substrate in $H_2{}^{18}O$ because of the nucleophilic addition of $H_2{}^{18}O$ on the side-chain nitrile of β-CNAla. After incubation, the D10N/L11K enzyme was denatured and digested with lysyl endopeptidase, where $H_2{}^{18}O$ was used as a solvent throughout these procedures. Since C-terminal carboxyl group produced by proteolysis contains two ^{18}O atoms when the proteolysis is performed in $H_2{}^{18}O$ (31), the peptide Gly-6–Lys-11 reconverted from the M'-18 peptide in $H_2{}^{18}O$ is expected to contain three ^{18}O atoms, two of which are in the carboxyl group of C-terminal Lys and the rest of which is in the side-chain amide group of Asn-10. The

hexapeptide isolated from D10N/L11K incubated without L-CPA and digested in $H_2{}^{18}O$ showed a new peak at *m/z* 653.4, which is about 4 Da higher than that derived from the unmodified one (Fig. 17E, M'+4). When the mutant enzyme was incubated in the presence of L-CPA, the mass spectrum showed a new peak at *m/z* 655.5, which is about 6 Da higher than that derived from the unmodified one (Fig. 17F, M'+6). These peaks were selected and further analyzed by tandem MS/MS. All the Y series ions produced from the M'+4 peptide shown in Fig. 18E were about 4 Da higher than the corresponding ions derived from the unmodified peptide shown in Fig. 18A. The Y series ions produced by fragmentations at the amino terminal side of Asn-10 in the M'+6 peptide were about 2 Da higher than the corresponding ions derived from the M'+4 peptide, whereas the molecular masses of C-terminal Lys derived from the two peptides were virtually identical (Fig. 18E and F). These results indicate that an ^{18}O atom occurred at Asn-10 specifically in the M'+6 peptide, and that the nitrile formed in the process of the structural change undergoes the nucleophilic attack of a water molecule to produce the side-chain amide of Asn-10.

In conclusion, the unique structural change of the D10N enzyme occurs through the mechanism shown in Scheme 8 (p.46): Asn-10 attacks the substrate to form the imidate, and a proton and D-lactic acid are eliminated for the formation of the nitrile. Thus the D10N enzyme itself as well as the wild-type enzyme produced by spontaneous deamidation catalyzes dehalogenation. This is the first report that the Asn substituted for nucleophile Asp functions as a catalytic nucleophile.

The Difference in Catalytic Efficiency Between Wild-type L-DEX YL and the D10N Mutant—I have found that the D10N mutant enzyme is spontaneously converted to the wild-type enzyme as described above. I have also shown that D10N itself catalyzes the dehalogenation through the mechanism shown in Scheme 8. Thus both of the D10N enzyme itself and the wild-type enzyme produced from D10N by hydrolytic deamidation contribute to the dehalogenation activity. This makes it difficult to determine the activity due to the D10N enzyme itself by measuring the concentration change of the substrate or that of the product. Accordingly, I have decided to determine the D10N activity based on the structural change of D10N itself. As shown in Fig. 16 (p.45), when the substrate is present abundantly (~ 18 min), a major part of D10N occurred as the M-18 variant, which has a nitrile group converted from the side-chain amide of Asn-10, indicating that the rate-limiting step of the reaction is the nucleophilic addition of water on the nitrile. Thus the D10N activity can be determined from the degradation rate of the nitrile. The decrease in relative height of the M-18 peak over the range from 30 to 60 min followed pseudo-first-order kinetics (Fig. 19A). The rate constant was found to be 2.94×10^{-4} sec^{-1}. The molecular activity of the wild-type enzyme was determined to be 47 sec^{-1} previously (15). These results indicate that the molecular activity of the wild-type enzyme is about 1.6×10^5 times as high as that of D10N. Thus a major part of the activity of the

D10N preparation observed in the standard assay mixture (about 1% of the wild-type enzyme activity for the fresh preparation of D10N) is due to the wild-type enzyme rather than the D10N enzyme itself: the D10N enzyme itself can account for only up to 0.0006% (= $1/(1.6 \times 10^5) \times 100$) of the wild-type enzyme activity.

The first step and the second step of the reaction catalyzed by the D10N enzyme (formation of the imidate intermediate and its conversion into the nitrile intermediate, respectively) proceed faster than the third step (hydrolysis of the nitrile intermediate).

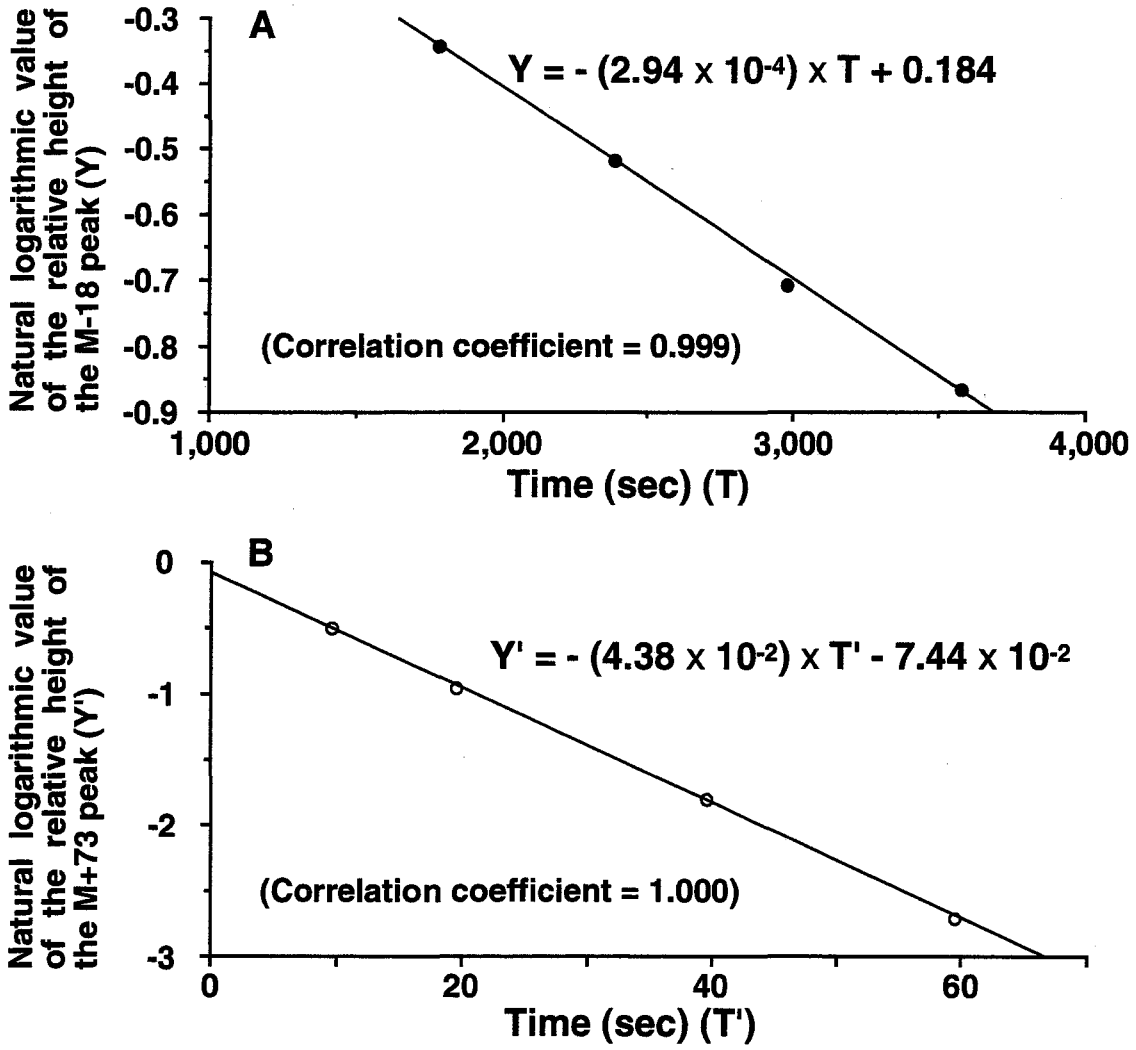

FIG. 19. **The rates of reconversion of the nitrile to the amide (A) and conversion of the imidate to the nitrile (B).** According to the mass spectral change shown in Fig. 16, the ratios of the peak height of M-18 to the sum of the peak heights of M-18 and M at 1,800 sec (30 min), 2,400 sec (40 min), 3,000 sec (50 min), and 3,600 sec (60 min) were 0.71, 0.596, 0.492, and 0.42, respectively (A); the ratios of the peak height of M+73 to the sum of the peak heights of M+73 and M-18 at 10 sec, 20 sec, 40 sec, and 60 sec were 0.6, 0.381, 0.164, and 0.066, respectively (B). These values were transformed to the natural logarithmic values. The plots of the transformed values against the time (sec) (A, •; B, o) were linear: correlation coefficient values were 0.999 (A) and 1.000 (B), respectively. From the inclination of these lines, the rate constants of the overall D10N reaction and the α,β-elimination of the imidate intermediate were determined to be 2.94×10^{-4} sec^{-1} (A) and 4.38×10^{-2} sec^{-1} (B), respectively.

The conversion rate of the imidate intermediate into the nitrile intermediate can be determined from the decrease in relative height of the M+73 peak over the range from 10 sec to 1 min, because there is virtually no peak of the native enzyme (M), which is a precursor of the imidate intermediate, and formation of the imidate intermediate is negligible (Fig. 16, p.45). The decrease in relative height of the M+73 peak in this time period followed first-order kinetics (Fig. 19B). The rate constant was found to be 4.38×10^{-2} sec^{-1}, which is larger than that of the nitrile hydrolysis by two orders of magnitude. The formation of the imidate intermediate proceeds so fast that it is impossible to determine its rate constant based on the mass spectral change shown in Fig. 16. It is supposed to be larger than that for the imidate degradation because accumulation of the imidate intermediate was observed as shown in Fig. 16.

DISCUSSION

Deamidation of Asn-10 of L-DEX YL D10N Mutant—Deamidation of Asn residues has been shown to occur in a variety of proteins either *in vitro* or *in vivo*. Two probable mechanisms for the deamidation have been reported. The first one involves formation of a succinimide intermediate and its hydrolysis to produce aspartyl residue as well as isoaspartyl residue in place of the Asn (74). The other probable mechanism has been mainly proposed for the deamidation of Asn mutagenetically substituted for Asp acting as a nucleophile in a wild-type enzyme. A water molecule is activated by a catalytic base of the mutant enzyme in the same manner as the water activation involved in the ester-intermediate hydrolysis in the wild-type enzyme reaction. The activated water directly attacks the side-chain amido-carbon of the Asn. This type of deamidation has been reported for DhlA D124N (67). I have shown in this chapter that Asn-10 mutagenetically substituted for the nucleophile Asp-10 of L-DEX YL is deamidated. The deamidation probably occurs in the same manner as DhlA D124N, although the deamidation rate of L-DEX YL D10N is considerably slower than that of DhlA D124N. A water molecule activated by Ser-175, Asn-177, and Asp-180 most likely attacks Asn-10 to deamidate it.

Mechanism of the Structural Change of Asn-10—In the X-ray structure of L-DEX YL S175A complexed with various L-2-chloroalkanoic acids, the carboxyl oxygens of the substrate are hydrogen-bonded with the Ser-118 hydroxyl group and the main-chain amido-nitrogens of Leu-11, Tyr-12, and Asn-119 (20). The hydrophobic pocket, which is mainly composed of side chains of Tyr-12, Gln-42, Leu-45, Phe-60, Lys-151, Asn-177, and Trp-179, exists around the alkyl group of the substrate. This pocket possibly plays an important role in stabilizing the alkyl group of the substrate through hydrophobic interactions, and also plays a role in determining the stereospecificity of the enzyme. The guanidino group of Arg-41 most likely serves as the halogen abstraction site. Because none of these amino acid residues were changed in D10N, the position of the substrate in the active site of D10N is probably

the same as that in the active site of wild-type L-DEX YL. The orientation of the amid-oxygen of Asn-10 is probably similar to that of the carboxyl oxygen of Asp-10 participating in the ester formation in the wild-type enzyme reaction: it points to the α-carbon atom of the substrate, whose electrophilicity is probably enhanced by Arg-41. Thus the side-chain amide of Asn-10 can attack the substrate to form the imidate in the D10N reaction in the same manner as the side-chain carboxylate of Asp-10 attacks the substrate to form the ester intermediate in the wild-type enzyme reaction.

D-Lactic acid is released from the ester intermediate by hydrolysis in the wild-type enzyme reaction. In contrast, in the D10N enzyme reaction, α,β-elimination of D-lactic acid and a proton, instead of hydrolysis, occurred as shown in Scheme 8 (p.46), even though a water molecule to be used for nitrile hydrolysis is probably present in the vicinity of the imidate. Why does not the imidate undergo hydrolysis instead of α,β-elimination in the D10N enzyme reaction as the ester intermediate does in the wild-type enzyme reaction? There are two possible reasons for this result. The first reason is that the electrophilicity of the imido-carbon of the imidate is lower than that of the carbonyl carbon of the ester: the nitrogen atom of the imidate is less electronegative than the oxygen atom of the carbonyl group, making the imido-carbon of the imidate less electrophilic. Accordingly, imido-carbon is less reactive with a nucleophilic water molecule. The second reason is the presence of a base that abstracts the imidate proton in the D10N enzyme to trigger the α,β-elimination of the imidate. This base is supposed to be Asp-180, which, in the wild-type enzyme, is suggested to function as a base to activate a water molecule for hydrolysis of the ester intermediate. This speculation is supported by the following observation: mass spectrum of the D10N/D180N double mutant enzyme incubated with L-CPA for 8 min showed two peaks at 26,177 Da (M") and 26,251 Da (M"+74), but no peak was observed at M"-18 (data not shown). The incubation time (8 min) is long enough for the D10N single mutant enzyme to accumulate as the M-18 variant. This result suggests that D10N/D180N can form an imidate intermediate, but cannot form a nitrile intermediate, supporting the view that Asp-180 plays a role in the α,β-elimination of the imidate.

Once the nitrile intermediate is produced, the proton abstracted from the imidate intermediate by Asp-180 is probably transferred to the nitrile nitrogen to enhance the electrophilicity of the nitrile carbon atom and to make Asp-180 competent to function as a base to activate the water molecule remaining in the vicinity of the nitrile. The activated water molecule is supposed to attack the nitrile-carbon atom to convert it to an amide.

Formation of free β-CNAla catalyzed by β-cyanoalanine synthase (EC 4.4.1.9) has been demonstrated in a wide range of organisms including higher plants (75, 76) and several species of bacteria (77, 78). However, the mechanism of the free β-CNAla synthesis is quite different from that of the β-CNAla residue formation report-

ed here: free β-CNAla is synthesized by β-replacement of the mercapto group in cysteine by cyanide (79), whereas the β-CNAla residue is formed by α,β-elimination of the imidate as shown in Scheme 8 (p.46).

Possible Roles and Occurrence of β-CNAla Residue in a Protein—Roy et al. have reported that replacement of the side-chain amide of Asn-5 of oxytocin by a nitrile produced an analog with a very weak activity, whereas a similar substitution in glycinamide-9 produced a highly active analog (80). Thus replacement of Asn with β-CNAla residue can alter functions of a protein. I have reported in this chapter that the side-chain amide of Asn residue in a protein can be reversibly converted to a nitrile. These results raise the possibility that Asn residue is posttranslationally converted into β-CNAla residue *in vivo* to modify the function of proteins. Although there has been no report on naturally produced β-CNAla residue in a protein so far, the presence of a β-CNAla residue has perhaps been unrecognized because of the lack of appropriate analysis method for amino acid residues constituting proteins: Edman degradation, the most widely used method for amino acid sequencing, results in the conversion of β-CNAla residue into PTH-Asn, thereby making it impossible to distinguish β-CNAla residue from Asn residue. Mass spectrometric analysis of proteins may reveal the presence of β-CNAla residue in various proteins in the future.

SUMMARY

L-DEX YL catalyzes the hydrolytic dehalogenation, in which Asp-10 acts as a nucleophile to attack the α-carbon of L-2-haloalkanoic acids to form an ester intermediate, which is hydrolyzed to produce D-2-hydroxyalkanoic acids. Replacement of Asp-10 by other amino acid residue such as Ala, Gly, Ser, or Glu results in total inactivation. In contrast, replacement by Asn is not the case: Asn-10 of the D10N mutant enzyme is spontaneously deamidated to yield Asp, though slowly, causing increasing activity of the D10N preparation. Thus the D10N preparation always contains a small amount of the wild-type enzyme, making it difficult to analyze the reaction involving the D10N enzyme itself by monitoring the degradation of the substrate. Accordingly, I have monitored the structural change of the D10N enzyme itself by ion-spray mass spectrometry during the reaction with the substrate: the small amount of the wild-type enzyme contaminating the enzyme preparation does not interfere with the mass spectra of the D10N enzyme itself, which constitutes a major part of the enzyme preparation. I have found that the D10N enzyme shows unique structural change when it was incubated with the substrate, L-CPA. LC/MS and tandem MS/MS analyses revealed that Asn-10 attacks the substrate to form an imidate, and a proton and D-lactic acid are eliminated to produce a nitrile (β-cyanoalanine residue), followed by hydrolysis to reproduce Asn-10. These findings demonstrate that the D10N mutant enzyme itself participates in dehalogenation. This is the first report of the function of Asn to catalyze nucleophilic substitution through its dynamic structural change including conversion to β-cyanoalanine residue as an intermediate structure.

CONCLUSION

The present study has been carried out to elucidate the reaction mechanisms of FAc-DEX and L-DEX YL.

On the basis of site-directed mutagenesis and ^{18}O-incorporation experiments, I have concluded that the reaction catalyzed by FAc-DEX proceeds through a two-step mechanism: Asp-105 first attacks the α-carbon of the substrate, causing the formation of an ester intermediate, which is subsequently hydrolyzed by a nucleophilic attack of a water molecule activated by His-272. Although little sequence similarity is found between FAc-DEX and L-DEX YL, the reaction mechanisms of the two dehalogenases are similar to each other in that their reactions proceed via an ester intermediate.

Extrinsic nucleophilic reagents such as hydroxylamine are expected to compete with an activated water in attacking the ester intermediate in the FAc-DEX and L-DEX YL reactions. In fact, both nucleophilic residues were paracatalytically modified by hydroxylamine. However, the modification of FAc-DEX was markedly different from that of L-DEX YL in two respects. First, Asp-105 of FAc-DEX was paracatalytically converted to an aspartate β-hydroxamic acid by hydroxylamine, whereas Asp-10 of L-DEX YL was converted to an aspartate β-hydroximate carboxyalkyl ester. Secondly, although L-DEX YL did not undergo paracatalytic inactivation by ammonia, which is less nucleophilic than hydroxylamine, FAc-DEX was paracatalytically inactivated by ammonia. In the latter case, Asp-105 was converted to Asn. These results suggest that the active site of FAc-DEX is mainly composed of hydrophobic residues and an ammonia molecule maintaining a lone electron pair to keep nucleophilicity is available at the active site. In fact, the three-dimensional structure model of FAc-DEX built by homology modeling using DhlA and BpoA2 as reference structures showed that the active site of FAc-DEX is characterized by a highly hydrophobic and basic environment.

Since Asp-105 of FAc-DEX and Asp-10 of L-DEX YL function as a catalytic nucleophile, replacement of these residues by other amino acid residues inactivate both enzymes. However, replacement by Asn is not the case in both enzymes. Asn-105 of FAc-DEX D105N was shown to undergo a spontaneous nucleophilic attack of an activated water molecule to be deamidated to yield Asp, causing increasing activity of the D105N preparation. Asn-10 of L-DEX YL D10N was also deamidated in the same manner as Asp-105 of FAc-DEX. Surprisingly, L-DEX YL D10N showed unique structural change when it was incubated with the substrate, L-CPA. Ion-spray mass spectrometric analyses revealed that Asn-10 attacks the substrate to form an imidate, and a proton and D-lactic acid are eliminated to produce a nitrile (β-cyanoalanine residue), which is subsequently hydrolyzed to reconvert into Asn-10. These findings demonstrate that L-DEX YL D10N itself participates in dehalogena-

tion. This is the first report of the function of Asn to catalyze nucleophilic substitution through its dynamic structural change including conversion to β-cyanoalanine residue as an intermediate structure.

ACKNOWLEDGMENTS

I wish to express my sincere gratitude to Dr. Nobuyoshi Esaki, Professor of the Laboratory of Microbial Biochemistry, Institute for Chemical Research, Kyoto University, for his kind guidance and generous encouragement throughout the course of this study.

I am deeply grateful to Dr. Tohru Yoshimura, Associate Professor of the Laboratory of Microbial Biochemistry, Institute for Chemical Research, Kyoto University, for his kindness and helpful suggestions.

I would like to express my gratitude to Dr. Tatsuo Kurihara, Research Associate of the Laboratory of Microbial Biochemistry, Institute for Chemical Research, Kyoto University, for his precise advice, valuable discussion, and warm encouragement through the course of this study.

I am greatly indebted to Dr. Kenji Soda, Professor Emeritus of Kyoto University, for his kind support and warm encouragement.

I am deeply grateful to Dr. Haruhiko Kawasaki, Professor of Department of Agricultural Chemistry, University of Osaka Prefecture, for his valuable support.

I am greatly indebted to Dr. Susumu Tsunasawa, Director of Protein Analysis Center of Takara Shuzo Co., Ltd., for his kind support and warm encouragement.

I would like to express my gratitude to Dr. Jun Hiratake, Associate Professor of the Laboratory of Chemistry of Molecular Biocatalysts, Institute for Chemical Research, Kyoto University, for his kind help and useful suggestions.

I am greatly indebted to Dr. Masaru Miyagi, Application Chemist of Biomedical Group of Takara Shuzo Co., Ltd., for his kind support and helpful suggestions.

I would like to express my gratitude to Mr. Yoshifumi Kogure, Application Chemist of Biomedical Group of Takara Shuzo Co., Ltd., for his generous support and warm encouragement.

I am greatly indebted to Dr. Yasuo Hata, Associate Professor of the Laboratory of Biopolymer Structure, Institute for Chemical Research, Kyoto University, for his kindness and helpful suggestions.

I am also indebted to Dr. Tomomi Fujii, Research Associate of the Laboratory of Biopolymer Structure, Institute for Chemical Research, Kyoto University, for his kind help and warm encouragement.

I am grateful to Ms. Toshiko Hirasawa, Ms. Mio Seki, Ms. Kumiko Nishikawa, and Ms. Machiko Utsunomiya for their kind help and warm encouragement.

I acknowledge the helpful comments and suggestions of my colleagues, especially Dr. Ji-Quan Liu, Dr. Yong-Fu Li, Dr. Chung Park, Dr. Andrey Galkin, and Dr. Hisaaki Mihara.

I am greatly indebted to Ms. Mieko Morishita, Chairperson of the Board of Directors of Morishita Jintan Co., Ltd., for her generous support.

I am grateful to Mr. Keiji Endo, Mr. Mitsuhiro Nishihara, Mr. Takuma Uo, Mr. Shin-ichiro Kato, Mr. Seung-Pyo Hong, Ms. Tasuku Watanabe, and Mr. Takahiro Yamauchi. They shared their valuable time with me and helped me during the course of this study.

I am also expressing my sincere thanks to Dr. Kwang-Hwan Jhee, Dr. Vincenzo Nardi-Dei, Dr. Sergey Gorlatov, Dr. Natasha Gorlatova, Dr. Yoichi Kurokawa, Dr. Kazuhisa Kishimoto, Dr. Li-Dong Liu, Dr. Aldo Gutierrez, Dr. Yoshihiro Fuchikami, Dr. Dong-Won Choo, Dr. Akira Watanabe, Mr. Takeshi Suzuki, Mr. Dong-Ho Seong, Mr. Yosuke Doi, Mr. Takeshi Kurono, Mr. Hitoki Miyake, Ms. Luda Kulakova, Mr. Kazuaki Yoshimune, Mr. Masaki Maeda, Mr. Kazuo Shiomi, Ms. Yuriko Hirano, Ms. Momoko Ueda, Mr. Sou Takeda, Mr. Tozo Nishiyama, Mr. Yun-Lin Wei, Mr. Daisuke Nakayama, Ms. Ayako Isui, Ms. Mami Saito, Ms. Fumiko Todo, Ms. Megumi Saito, Mr. Hiroyuki Takahata, Ms. Michiko Nakano, Mr. Kensuke Mori, Mr. Robert Alexander John Douglas Kennedy, Ms. Geok-Yong Yow, Mr. Mehran Miroliaei, and all the other members of the Laboratory of Microbial Biochemistry, Institute for Chemical Research, Kyoto University, at both past and present, for sharing their valuable time and encouraging me.

Finally, I wish to express my hearty gratitude to my parents and sisters for their immense understanding and warm encouragement.

REFERENCES

1. Bantleon, R., Altenbuchner, J., and van Pée, K.-H. (1994) *J. Bacteriol.* **176,** 2339–2347
2. van Schijndel, J. W. P. M., Vollenbroek, E. G. M., and Wever, R. (1993) *Biochim. Biophys. Acta.* **1161,** 249–256
3. Facey, S. J., Groß, F., Vining, L. C., Yang, K., and van Pée, K.-H. (1996) *Microbiology* **142,** 657–665
4. Baron, M. L., Bothroyd, C. M., Rogers, G. I., Staffa, A., and Rae, I. D. (1987) *Phytochemistry* **26,** 2293–2295
5. Tamura, T., Wada, M., Esaki, N., and Soda, K. (1995) *J. Bacteriol.* **177,** 2265–2269
6. Richard, A. M., and Hunter, E. S. 3rd. (1996) *Teratology* **53,** 352–360
7. Akers, K. S., Sinks, G. D., and Schultz, T. W. (1999) *Environ. Toxicol. Pharmacol.* **7,** 33–39
8. Fetzner, S. (1998) *Appl. Microbiol. Biotechnol.* **50,** 633–657
9. Molina, M. J., and Rowland, F. S. (1974) *Nature* **249,** 810–812
10. Longstreth, J. (1988) *Cancer Metastasis Rev.* **7,** 321–333
11. Taylor, H. R., West, S. K., Rosenthal, F. S., Munoz, B., Newland, H. S., Abbey, H., and Emmett, E. A. (1988) *N. Engl. J. Med.* **319,** 1429–1433
12. Liu, J.-Q., Kurihara, T., Hasan, A. K. M. Q., Nardi-Dei, V., Koshikawa, H., Esaki, N., and Soda, K. (1994) *Appl. Environ. Microbiol.* **60,** 2389–2393
13. Swanson, P. E. (1999) *Curr. Opin. Biotechnol.* **10,** 365–369
14. Nardi-Dei, V., Kurihara, T., Okamura, T., Liu, J.-Q., Koshikawa, H., Ozaki, H., Terashima, Y., Esaki, N., and Soda, K. (1994) *Appl. Environ. Microbiol.* **60,** 3375–3380
15. Kurihara, T., Liu, J.-Q., Nardi-Dei, V., Koshikawa, H., Esaki, N., and Soda, K. (1995) *J. Biochem.* **117,** 1317–1322
16. Liu, J.-Q., Kurihara, T., Miyagi, M., Esaki, N., and Soda, K. (1995) *J. Biol. Chem.* **270,** 18309–18312
17. Liu, J.-Q., Kurihara, T., Miyagi, M., Tsunasawa, S., Nishihara, M., Esaki, N., and Soda, K. (1997) *J. Biol. Chem.* **272,** 3363–3368
18. Hisano, T., Hata, Y., Fujii, T., Liu, J.-Q., Kurihara, T., Esaki, N., and Soda, K. (1996) *J. Biol. Chem.* **271,** 20322–20330
19. Ollis, D. L., Cheah, E., Cygler, M., Dijkstra, B., Frolow, F., Franken, S. M., Harel, M., Remington, S. J., Silman, I., Schrag, J., Sussman, J. L., Verschueren, K. H. G., and Goldman, A. (1992) *Protein Eng.* **5,** 197–211
20. Li, Y.-F., Hata, Y., Fujii, T., Hisano, T., Nishihara, M., Kurihara, T., and Esaki, N. (1998) *J. Biol. Chem.* **273,** 15035–15044

21. Li, Y.-F., Ichiyama, S., Kurihara, T., Miyagi, M., Tsunasawa, S., and Esaki, N. (in preparation)
22. Pries, F., Kingma, J., Pentenga, M., van Pouderoyen, G., Jeronimus-Stratingh, C. M., Bruins, A. P., and Janssen, D. B. (1994) *Biochemistry* **33,** 1242–1247
23. Yang, G., Liang, P.-H., and Dunaway-Mariano, D. (1994) *Biochemistry* **33,** 8527–8531
24. Crooks, G. P., Xu, L., Barkley, R. M., and Copley, S. D. (1995) *J. Am. Chem. Soc.* **117,** 10791–10798
25. Hill, K. E., Marchesi, J. R., and Weightman, A. J. (1999) *J. Bacteriol.* **181,** 2535–2547
26. Verschueren, K. H. G., Seljée, F., Rozeboom, H. J., Kalk, K. H., and Dijkstra, B. W. (1993) *Nature* **363,** 693–698
27. Pries, F., Kingma, J., Krooshof, G. H., Jeronimus-Stratingh, C. M., Bruins, A. P., and Janssen, D. B. (1995) *J. Biol. Chem.* **270,** 10405–10411
28. Kennes, C., Pries, F., Krooshof, G. H., Bokma, E., Kingma, J., and Janssen, D. B. (1995) *Eur. J. Biochem.* **228,** 403–407
29. Schanstra, J. P., and Janssen, D. B. (1996) *Biochemistry* **35,** 5624–5632
30. Nardi-Dei, V., Kurihara, T., Park, C., Esaki, N., and Soda, K. (1997) *J. Bacteriol.* **179,** 4232–4238
31. Nardi-Dei, V., Kurihara, T., Park, C., Miyagi, M., Tsunasawa, S., Soda, K., and Esaki, N. (1999) *J. Biol. Chem.* **274,** 20977–20981
32. Goldman, P. (1969) *Science* **164,** 1123–1130
33. Goldman, P. (1965) *J. Biol. Chem.* **240,** 3434–3438
34. Tonomura, K., Futai, F., Tanabe, O., and Yamaoka, T. (1965) *Agric. Biol. Chem.* **29,** 124–128
35. Kawasaki, H., Miyoshi, K., and Tonomura, K. (1981) *Agric. Biol. Chem.* **45,** 543–544
36. Kawasaki, H., Tone, N., and Tonomura, K. (1981) *Agric. Biol. Chem.* **45,** 29–34
37. Peters, R. A. (1957) *Adv. Enzymol.* **18,** 113–159
38. Lauble, H., Kennedy, M. C., Emptage, M. H., Beinert, H., and Stout, C. D. (1996) *Proc. Natl. Acad. Sci. USA* **93,** 13699–13703
39. Kawasaki, H., Yahara, H., and Tonomura, K. (1984) *Agric. Biol. Chem.* **48,** 2627–2632
40. Goldman, P., Milne, G. W. A., and Keister, D. B. (1968) *J. Biol. Chem.* **243,** 428–434
41. Lacourciere, G. M., and Armstrong, R. N. (1993) *J. Am. Chem. Soc.* **115,** 10466–10467
42. Tzeng, H.-F., Laughlin, L. T., and Armstrong, R. N. (1998) *Biochemistry* **37,** 2905–2911

43. Kurihara, T., Nardi-Dei, V., Park, C., Esaki, N., Soda, K., Tsunasawa, S., and Miyagi, M. (1997) *Mechanisms of biohalogenation and dehalogenation* (Janssen, D. B. et al., ed.) pp.167–174, Royal Netherlands Academy of Arts and Sciences, Amsterdam, the Netherlands
44. Sambrook, J., Fritsch, E. F., and Maniatis, T. (1989) *Molecular Cloning–A Laboratory Manual*, 2nd ed., Cold Spring Harbor, NY
45. Kawasaki, H., Tsuda, K., Matsushita, I., and Tonomura, K. (1992) *J. Gen. Microbiol.* **138,** 1317–1323
46. Kunkel, T. A., Roberts, J. D., and Zakour, R. A. (1987) *Methods Enzymol.* **154,** 367–382
47. Iwasaki, I., Utsumi, S., Hagino, K., and Ozawa, T. (1956) *Bull. Chem. Soc. Jpn.* **29,** 860–864
48. Janssen, D. B., Pries, F., van der Ploeg, J., Kazemier, B., Terpstra, P., and Witholt, B. (1989) *J. Bacteriol.* **171,** 6791–6799
49. Wang, Z., Asenjo, A. B., and Oprian, D. D. (1993) *Biochemistry* **32,** 2125–2130
50. Jönsson, B. M., Håkansson, K., and Liljas, A. (1993) *FEBS Lett.* **322,** 186–190
51. Qian, M., Haser, R., and Payan, F. (1993) *J. Mol. Biol.* **231,** 785–799
52. Gregg, K., Hamdorf, B., Henderson, K., Kopecny, J., and Wong, C. (1998) *Appl. Environ. Microbiol.* **64,** 3496–3498
53. Christen, P. (1977) *Methods Enzymol.* **46,** 48–54
54. Gupta, S., Hollenstein, R., Kochhar, S., and Christen, P. (1993) *Eur. J. Biochem.* **214,** 515–519
55. Markovic-Housley, Z., Schirmer, T., Hohenester, E., Khomutov, A. R., Khomutov, R. M., Karpeisky, M. Y., Sandmeier, E., Christen, P., and Jansonius, J. N. (1996) *Eur. J. Biochem.* **236,** 1025–1032
56. Shao, Y., Xu, M.-Q., and Paulus, H. (1996) *Biochemistry* **35,** 3810–3815
57. Howard, S., He, S., and Withers, S. G. (1998) *J. Biol. Chem.* **273,** 2067–2072
58. Hecht, H. J., Sobek, H., Haag, T., Pfeifer, O., and van Pée, K.-H. (1994) *Nat. Struct. Biol.* **1,** 532–537
59. Sali, A., and Blundell, T. L. (1993) *J. Mol. Biol.* **234,** 779–815
60. Rost, B. (1997) *Proteins* **Suppl. 1,** 192–197
61. Laskowski, R. A., MacArthur, M. W., Moss, D. S., and Thornton, J. M. (1993) *J. Appl. Crystallogr.* **26,** 283–291
62. Bowie, J. U., Lüthy, R., and Eisenberg, D. (1991) *Science* **253,** 164–170
63. Caplow, M., and Jencks, W. P. (1964) *J. Biol. Chem.* **239,** 1640–1652
64. Nishino, T., Kozarich, J. W., and Strominger, J. L. (1977) *J. Biol. Chem.* **252,** 2934–2939
65. Burdette, R. A. and Quinn, D. M. (1986) *J. Biol. Chem.* **261,** 12016–12021

66. Kraulis, P. J. (1991) *J. Appl. Crystallogr.* **24,** 946–950
67. Pries, F., Kingma, J., and Janssen, D. B. (1995) *FEBS Lett.* **358,** 171–174
68. Laughlin, L. T., Tzeng, H.-F., Lin, S., and Armstrong, R. N. (1998) *Biochemistry* **37,** 2897–2904
69. Xiang, H., Dong, J., Carey, P. R., and Dunaway-Mariano, D. (1999) *Biochemistry* **38,** 4207–4213
70. Wakabayashi, S., and Matsubara, H. (1995) *Theory and Practice on Enzymes and Other Proteins* (Horio, T., 2nd ed.) pp.467–474, Nankodo, Japan
71. Tarr, G. E. (1977) *Methods Enzymol.* **47,** 335–357
72. Tennant, G. (1979) *Comprehensive Organic Chemistry* (Barton, D. and Ollis, W. D., ed.) **Vol. 2** (Sutherland, I. O., ed.), pp.490–495, Pergamon Press, UK
73. Sykes, P. (1986) *A Guidebook to Mechanism in Organic Chemistry* (6th ed.) pp.244–245, Longman Scienfic & Technical, UK
74. Stephenson, R. C., and Clarke, S. (1989) *J. Biol. Chem.* **264,** 6164–6170
75. Akopyan, T. N., Braunstein, A. E., and Goryachenkova, E. V. (1975) *Proc. Natl. Acad. Sci. USA* **72,** 1617–1621
76. Maruyama, A., Ishizawa, K., Takagi, T., and Esashi, Y. (1998) *Plant. Cell Physiol.* **39,** 671–680
77. Dunnill, P. M., and Fowden, L. (1965) *Nature* **208,** 1206–1207
78. Castric, P. A., and Conn, E. E. (1971) *J. Bacteriol.* **108,** 132–136
79. Tolosa, E. A., Maslova, R. N., Goryachenkova, E. V., Willhardt, I. H., and Braunstein, A. E. (1975) *Eur. J. Biochem.* **53,** 429–436
80. Roy, U., Gazis, D., Dal Pan, G., Schwartz, I. L., and Roy, J. (1983) *Int. J. Pept. Protein Res.* **22,** 525–538